AD-A036 494   UNIVERSITY OF MANCHESTER INST OF SCIENCE AND TECHNOLO--ETC F/G 4/1
            ATMOSPHERIC AEROSOL RESEARCH AT UMIST.(U)
   DEC 76   J LATHAM, M J GAY   DA-ERO-124-74-G-0032

UNCLASSIFIED   NL

| OF |
ADA036494

END

DATE
FILMED
3-77

MICROCOPY RESOLUTION TEST CHART

NATIONAL BUREAU OF STANDARDS-1963-A

AD _____

⑫
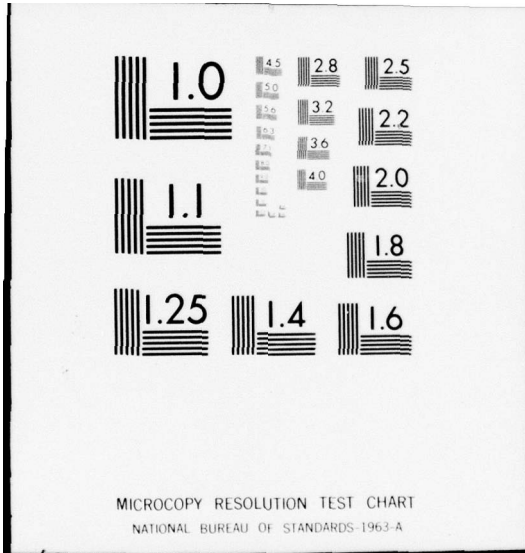
ATMOSPHERIC AEROSOL RESEARCH AT UMIST

Final Technical Report

COPY AVAILABLE TO DDC DOES NOT PERMIT FULLY LEGIBLE PRODUCTION

DDC RECEIVED MAR 7 1977 C

European Research Office

United States Army

Research and Development Group, Europe

London, United Kingdom

Contract Number DA-ERO-124-74-G0023 32

Department of Pure and Applied Physics

University of Manchester Institute of Science and Technology

Manchester, ENGLAND.

December 1976

Dr M J Gay
Research Scientist

Professor J Latham
Principal Investigator

REPORT DOCUMENTATION PAGE		READ INSTRUCTIONS BEFORE COMPLETING FORM
1. REPORT NUMBER	2. GOVT ACCESSION NO.	3. RECIPIENT'S CATALOG NUMBER
4. TITLE (and Subtitle) Atmospheric Aerosol Research at UMIST.		5. TYPE OF REPORT & PERIOD COVERED Final Technical Report March 76 — December 76
		6. PERFORMING ORG. REPORT NUMBER
7. AUTHOR(s) Professor J. Latham Dr. M.J. Gay		8. CONTRACT OR GRANT NUMBER(s) DAERO-124-74-G-0032
9. PERFORMING ORGANIZATION NAME AND ADDRESS Department of Pure & Applied Physics University of Manchester Inst. of Science & Technology, Manchester, U.K. (England)		10. PROGRAM ELEMENT, PROJECT, TASK AREA & WORK UNIT NUMBERS 6-11-02A-DM1611 02B53B-00-472
11. CONTROLLING OFFICE NAME AND ADDRESS US Army R&S Gp (Eur) Box 65, FPO NY 09510		12. REPORT DATE December 1976
		13. NUMBER OF PAGES 66
14. MONITORING AGENCY NAME & ADDRESS(if different from Controlling Office) John Latham M. J. Gay		15. SECURITY CLASS. (of this report) UNCLASSIFIED
		15a. DECLASSIFICATION/DOWNGRADING SCHEDULE

16. DISTRIBUTION STATEMENT (of this Report)

APPROVED FOR PUBLIC RELEASE - DISTRIBUTION UNLIMITED

17. DISTRIBUTION STATEMENT (of the abstract entered in Block 20, if different from Report)

DM161102B53B

D D C
RECEIVED
MAR 7 1977
A

18. SUPPLEMENTARY NOTES

19. KEY WORDS (Continue on reverse side if necessary and identify by block number)
AEROSOL:

20. ABSTRACT (Continue on reverse side if necessary and identify by block number)
This report describes the work carried out during the first three years of research devoted to aerosol studies, both in the UMIST laboratories and particularly at the field station at Great Dunn Fell (847 m a s l) in Cumbria.

Some preliminary measurements have been made primarily to ensure the accurate and reliable operation of the various devices installed rather than with any closely defined specific scientific goals in mind at this time. However, two

specific aerosol projects have been conducted during this period. The former project is a laboratory investigation of the effects of mixing on the evolution of wet aerosol spectra, and the latter project deals with electrical studies of the turbulent mixing of aerosol trapped at a temperature inversion. These studies are described in detail in sections 3 and 4.

The final section of this report briefly describes and discusses recent work carried out and likely future developments.

CONTENTS

LEGENDS TO FIGURES

LEGENDS TO TABLES

1. INTRODUCTION

This report describes the work carried out during the first three years of research devoted to aerosol studies, both in the UMIST laboratories and particularly at our field station at Great Dun Fell (847 m a s l) in Cumbria. Of necessity, a considerable amount of time and effort has been devoted to the design, construction, installation and calibration of equipment, particularly at the latter site and it is considered worthwhile describing the comprehensive facilities which now exist there in some detail. This decription forms the basis of Section 2.

Some preliminary measurements have been made primarily to ensure the accurate and reliable operation of the various devices installed rather than with any closely defined specific scientific goals in mind at this time. However, two specific aerosol projects have been conducted during this period. The former project is a laboratory investigation of the effects of mixing on the evolution of wet aerosol spectra, and the latter project deals with electrical studies of the turbulent mixing of aerosol trapped at a temperature inversion. These studies are described in detail in sections 3 and 4.

The final section of this report briefly describes and discusses recent work carried out and likely future developments

2. THE GREAT DUN FELL RESEARCH STATION, AND ASSOCIATED FACILITIES

2.1 Introduction

The UMIST Field Research Station is situated on the summit of Great Dun Fell, in Cumbria, (Fig 2.1). The facilities comprise a stone building, situated 847 metres above sea level with adjoining concrete forecourt for the disposition of ground-based instrumentation and an adjacent wooden mast upon which instruments can be mounted up to a height of 20m above the ground. The site is generally accessible throughout the year by Land Rover, although in extreme winter conditions a snow cat is occasionally required. To avoid daily wastage of time through travel between the site and UMIST (a journey of approximately $2\frac{1}{2}$ hours) a caravan is located at the foot of the Fell; in addition, facilities for overnight accommodation exist at the station itself.

The building it equipped with heating, lighting, and telephone. A water tank and toilet have been installed together with cooking and other domestic facilities. Thus the station can be continuously manned for periods of several days at a time.

A large laboratory area has been fitted out with extensive bench space and ample mechanical and electronic equipment to permit onsite construction, modification or maintenance of apparatus when this is necessary. Traversing the laboratory at one end is a cloud duct which provides a convenient means of sampling the external environment

A comprehensive and flexible range of data recording
equipment has been installed which we believe to be capable
of meeting all our requirements; this facility includes
a 12 channel UV recorder; a 15 channel data logger; a
multichannel digital tape recorder; three digideck recorders;
and domestic cassette recorders for use in conjunction
with individual experiments. The latter four systems all
store data in a manner compatable with our PDP-8e computer
at UMIST for convenient subsequent analysis.

The Great Dun Fell station, by virtue of its location,
has several highly advantageous features. Because of its
altitude it is frequently in cloud - for part of approximately
250 days each year. Also its location and the prevailing
winds are such that it is generally not exposed to local
sources of pollution. For these reasons apparatus has
been installed to measure and record a wide range of atmos-
pheric particulates, both solid and liquid.

Measurement of Aitken Nuclei

The concentration of Aitken nuclei is determined using
a photoelectric nucleus counter of the type described by
Metnieks and Pollak (1959). Pollak and his co-workers
have carried out extensive investigations on the accuracy
and reliability of these devices and their performance
is well-known and documented. Two counters are operated
in parallel, Figure 2.2, and the system is semi-automated
by the use of electrical solenoid valves operated by an
electromechanical timer. Air is sampled from the cloud duct,
either directly to the counters, to determine the total
concentration of nuclei or via concentric cylindrical

denuders across which the potential may be varied to
selectively descrimirate against particles of different
mobilities. In this way an indication of the size distri-
bution within the total concentration of nuclei may be
determined. Alternatively, the denuders may be employed
with the photoelectric nucleus counters to determine the
total number of nuclei and the total number of uncharged
particles. Provided that the aerosol is in electrical
equilibrium and that the charge distribution on the popu-
lation of aerosol particles follows Boltzmann's Law an
average size may be determined for the population.
Electrical equilibrium of the aerosol may be assured by
passing the aerosol over a weak radioactive source.
The average size, as deduced from the measured fraction
of the uncharged nuclei in the actual aerosol is in fact
the size of an equivalent monodisperse aerosol. (Rich,
 Pollak and Metnieks, 1959).

The signals from the counters are suitably processed
and recorded on the data logger, which provides a punched
tape output. The data is returned to UMIST for subsequent
analysis by a PDP-8e computer.

In principle, the photoelectric nucleus counter registers
all Aitken nuclei (10^{-7}cm $< r < 10^{-5}$cm) upon which conden-
sation may be achieved by the supersaturation resulting
from the expansion ratio of 1.21:1. (A higher expansion
ratio would result in condensation on small ions.) However,
in practice, this size range is limited, at the upper
end by gravitational settling of the largest droplets
formed in the counter, and at the lower end by losses due
to diffusion of the smaller particles in the interconnecting

tubing between cloud duct and counter. Fortunately,
expressions for the diffusion of aerosols in laminar
flow have been found for such situations (Gormley and
Kennedy, 1949), and corrections may be made to the raw
data to allow for these errors. By way of illustration,
for particles of radius 10^{-7} cm passing into the counter
at the normal operating flow rate (4 l min^{-1}), the ratio
of particles reaching the counter to those present at
the entrance $n/n_0 \approx 70\%$, and of those particles reaching
the counter a further 25% may be expected to diffuse to
the walls of the counter prior to detection. Fortunately,
the magnitude of these losses decreases rapidly with
increasing particle size, and suitable corrections to
the data are conveniently made during data analysis
with the PDP-8e.

Observations of Aitken nuclei concentration are most
conveniently expressed as a cumulative frequency distri-
bution, in which the logarithm of particle concentration
is plotted against the percentage of observations less
than a given value of particle concentration. Representative
results are given in figure 2.3. The experimental points
have been omitted from this figure for the sake of clarity.
Preliminary results reported in, for example, the interim
report for December 1975 have indicated the very small
amount of scatter in the results. When displayed in this
manner it is readily apparent that the distribution of
number concentration is well approximated by a log-normal
curve which provides a convenient means of parameterizing
the distribution terms of the geometric mean, Z_g and the

2.iv

geometric standard deviation σ_g. These parameters, together with the relavent details of mean wind speed and direction are summarised in Table 2.1.

Table 2.1: Variations in Aitken Nuclei Concentration at GDF

Curve	Wind Direction	Mean Wind Speed(kts)	Z_g cm^3.	σ_g	Remarks
A	045°	12	880	1.59	weekend sampling period clear air
B	210°	25	1550	1.35	clear air, cloud below station
C	210°	34	1780	1.83	In cloud
D	155°	35	1970	1.14	In clear air
E	190°	12	2250	1.38	In cloud
F	210°	31	2450	1.39	In cloud
G	235°	23	2650	2.79	In clear air local pollution (vehicular)
H	270°	15	2900	1.24	Local pollution source (standby generator)
J	240°	9	6500	1.38	Local Pollution source (gypsum)

The range of variation in Z_g is generally small (curves B-H inclusive) and the absolute value consistant with the nature of the location. Extreme values of Z_g (curves A and J) are readily explainable in terms of the incidence of anthropogenic sources of pollution.

The only fixed local source of pollution is a gypsum mine
located 8 km distant from the station on a bearing of
240°. Vehicular activity or the operation of the diesel
standby generator at GDF are readily apparent as signi-
ficant departures from the customary diurnal variation.
The occurence of other short-term fluctuations (typically
an increase in concentration of up to an order of magni-
tude for a period of $\sim$ 30 minutes) has been reported in
a previous interim report. The nature of the cause of
these aromolous fluctuations remains uncertain. We intend
to continue the systemmatic accumulation of data to provide
a statistically significant "benchmark" of Aitken nuclei
concentration under various prevailing meteorological conditions

2.3 Measurement of Giant Dry Aerosol by Inertial Impaction

The measurement of number concentration and size
distribution of particles $> 10^{-5}$cm is of particular interest
since these particles are precisely those which contribute
to low visibilities. To investigate this size range five
double-stage impactors of the type described by Jaenicke
(1971) were installed at GDF early in the research period.
Much useful imformation on the operation of the devices
was supplied by Dr R Reiter of the Physikalisch-
Bioklimatische Forschungstelle der Fraunhofer-Gesellschaft,
Garmsich-Partenkirchen, who is currently working on an
automated counting technique using an optoelectronic
method. (counting is performed at present by conventional
microscopy). In order to be able to obtain accurate measure-
ments of size distribution it is essential that the col-
lection efficiency of the individual second stages be

precisely known. These may be calculated by consideration
of the aerodynamics in the region of the nozzle, and are
found to be a sensitive function of the mean particle
density. The variation of particle diameter at peak
collection efficiency for the five double stage impactors
for a range of mean particle densities is given in Table 2.2

Table 2.2: Calculated Values of Particle Diameter of
Maximum collection efficiency for various
mean particle densities.

Mean Particle density g cm^{-3}	Particle Diameter d μm				
	Stage 1	Stage 2	Stage 3	Stage 4	Stage 5
0.65	0.337	0.628	1.30	2.79	6.38
1.00	0.233	0.461	0.972	2.09	4.75
2.00	0.146	0.291	0.623	1.355	3.05

With the optical microscopy techniques available to
us, we were only able to accurately determine particle sizes
d ⪆ 1.0 μm. Consequently by examination of the deposits
from stages 4 and 5 only were we able to determine that
the calibration most closely corresponding to our measure-
ments was for a mean particle density of 1.0 gm cm^{-3}.

In order to accurately determine number concentration
it is necessary to know the magnitude of the peak collec-
tion efficiency η. A comparison of both theoretical cal-
culations as well as experimental determinations published
in the literature shows considerable discrepancies.

Jaenicke and Blifford (1974) have reviewed this subject, and suggested likely causes for the discrepancies. However, in view of the uncertainties concerning the obtainable accuracy of number concentrations and size distributions of atmospheric aerosols, together with the inordinately time-consuming nature of the data analysis, it was deemed advisable to postpone making these measurements until the acquisition of the optical scattering particle counter described in the next section.

The theory of inertial deposition employed to determine the collection efficiency of each stage of the impactors demands that the size of particle captured is actually an "equivalent aerodynamic size", rather than some specific linear dimension, whether real or derived, in order to account for variations in parameters such as shape, density and drag coefficient of the particles. It is, therefore, of interest to examine the range of shapes and sizes for which a given impactor stage is descriminative.

As a consequence of these considerations, it was felt that examination of the samples obtained by the impactors by scanning electron microscopy (SEM) techniques could be instructive. To this end, the microscope slides normally employed were replaced by metal blanks of identical size, at the centre of which a hole was machined to accept a standard SEM sample stage. Care was taken to maintain the face of the SEM sample stage flush with the supporting metal blank to minimise disturbance of the airflow in the critical region of the impactor jet, so that samples would be representative of those obtained under normal operating conditions.

Examination of the photographs thus obtained (typical examples of which were included in the interim report for June 1976) disclosed considerable variations in particle shape and size for any given impactor stage. The variations in overall size were enhanced by the fact that many of the larger particles were clearly agglomerates. Many small particles at extreme magnification were clearly crystalline in nature. This variability in the nature of particles gives rise to considerable uncertainty in the value of mean particle density.

2.4 Measurement of Giant Aerosol by Optical Scattering

During the latter part of the research period we acquired a Royco Model 225 Aerosol Particle Monitor with an autoscan digital display module 508 and Model 241 sensor. This device has been installed at the GDF field station and is currently undergoing commissioning and calibration. The counter is precalibrated with monodisperse sources of latex particles in five radii catagories: 0.25-0.35, 0.35-0.7, 0.7-1.4, 1.4-3.0 and 3.0-5.0um. Since the calibration is sensitive to the refractive index of the aerosol being.measured, we have deemed it desirable to check the calibration for natural aerosol particles.

2.5 Atmospheric Particulate Collector

One further device for sampling dry atmospheric particulates is described briefly here for completeness. This is the atmospheric particulate collector designed by ASL at WSMR. In this device, air to be sampled is drawn up and into the top of the cylindrical body through circumferential orifices and then passes down

the body to a filter mounted in a Gelman filter holder
at the base of the body. The device is aspirated by a
Reciprotor type R506 pump such that the flow rate into
the intake is sufficiently high to overcome the sedimenta-
tion effects of gravity but not so high that particle
inertia effects become serious enough to cause the particles
to deviate from the flow stream.

Two such devices are currently being operated, one
at UMIST in a densely populated urban environment, and
the other at GDF.

2.6 Measurement of Giant Wet Aerosol

In order to determine the size distribution of giant
wet aerosol an electrostatic-disdrometer has been construc-
ed and tested, both in natural and laboratory conditions.
The calibration programme has bee both detailed and exten-
sive in view of the discrepancies in the behaviour of
similar devices reported in the scientific literature.

A block diagram of the present system is shown in
Figure 2.4. Essentially, pulses from the Keily Probe,
together with the output from the hot-wire liquid water
content device, are processed and recorded on a domestic
cassette recorder at the field station. The tapes are
then returned to UMIST and played back via the necessary
ancillary circuitry, into the PDP-8e computer. The computer
is programmed to accept pulses, sort into channels and
output the total and channel counts to the digistore.
Cloud liquid water content is read at the beginning and
end of each histogram and also output to the digistore.

The raw data thus available from the digistore may then be fed to the PDP-8e which is reprogrammed and run to output actual histograms of size distribution to the teletype. The data is available either digitally or plotted out in suitable format, and provides in addition to size distribution, total count, total liquid water content (ie $\sum\limits_{i} nr^3$), the mean radius, dispersion, peak channel size, count and liquid water content and pre- and post run liquid water content derived from the hot-wire device. Typically, a single histogram is complied for 2000 pulses or twenty seconds of data. Various system status checks and monitoring facilities are available. Provision has been made in this latter programme to incorporate a correction factor for each channel of the histogram once the collection efficiency of the Keily Probe has been determined as a function of droplet size.

Calibration of the Keily Probe has been carried out in these laboratories using a specially constructed wind tunnel capable of ventilating the probe at speeds up to 25 m sec^{-1}. The air is initially drawn through a humidifier and then droplets are introduced into the airstream from a 'spinning top' generator.

The droplet spectrum available from this device may be selectively broad or narrow. It is determined by insertion of magnesium oxide coated glass rods of known collection efficiency into the air stream. In this manner, the preliminary calibration curve presented in a previous interim report has been corroborated. The integrated Keily probe output and the hot-wire liquid water content device have been calibrated. Agreement between the two

was found to be excellent; the linearity of the output
from the hot-wire device was also good. A laboratory
determination of the collection efficiency of the probe
is currently being made.

2.7 Pollutant Scavenging by Raindrops

The distribution, with raindrop size and time, of
various pollutants in rainfall is being studied to gain
information about the entrainment of aerosols in rain.
The technique employed utilises a collecting raindrop
disdrometer (Georgii and Wotzel, 1970) and analysis of
the collected samples by electrochemical techniques using
ion-sensitive electrodes. Using this technique, concen-
trations of selected ions as low as 1 ppm may be deter-
mined for sample volumes as small as 0.3 ml. This study
will be augmented by precise determination of the raindrop
size distribution using a novel design of disdrometer
developed at UMIST, specifically suited to obtaining
accurate results in the generally high prevailing wind
conditions at GDF. In addition, electrochemical analysis
of the samples obtained by the double stage impactors
is planned.

3. LABORATORY STUDIES OF THE EFFECTS OF MIXING ON THE

EVOLUTION OF WET AEROSOL SPECTRA

3.1 Introduction

The evolution of droplet populations formed by condensation in fogs and clouds has been studied, experimentally and theoretically, by many workers. The most detailed and reliable information on cumulus clouds of moderate depth, has been provided by the airborne investigations conducted, presented and discussed by Warner (1969a,b, 1970, 1973a,b).

In these papers Warner points to important inter-related features of the shape and development of the droplet spectrum – prior to the onset of a significant contribution from coalescence – which he is unable to explain quantitatively. These are that (1) droplets of the smallest detectable size (diameter $d \sim 5\mu m$) are found at all levels within the clouds, irrespective of the distance from the vertical boundaries; (2) the droplet spectrum is consequently broad, and is commonly found to be bimodal; (3) the dispersion of the spectrum – defined as the ratio of the standard deviation to the mean diameter – is typically around 0.2 near the cloud base, and increases at higher levels.

Warner (1969b) showed that the spectral shape and dispersion near cloud base can be explained if account is taken of the fact that the condensation coefficient for water vapour molecules is consider-

ably less than 1. His papers provide convincing evidence
for the association of the other spectral features alluded
to with mixing between cloud and undersaturated environ-
mental air. However, detailed calculations (Warner,1973a),
in which entrainment of undersaturated environmental air
was considered, yielded evolving spectra quite unlike
those observed. This led Warner to conclude that "simple
mixing between the cloud and the environment is unimport-
ant is determining the droplet size distribution, at
least in the early stages of cloud growth".

On the other hand, Mason and Jonas (1974) and
Jonas and Mason (1974) have presented calculations, based
on a multi-thermal model of the air flow, from which they
conclude that the major features of the droplet spectra
can be explained in terms of mixing between the cloud
and its environment. This conclusion has been challenged
by Warner (1975) who argues that the dynamics, thermo-
dynamics and microphysics employed in these calculations
are unrealistic. The calculations have been defended
by Mason (1975), but it is clear that no consensus of
agreement exists as to the reasons for the particular
features of cloud droplet spectra to which Warner has
drawn our attention.

In the present work experiments are described which
were designed to study the effect on a population of
droplets formed by condensation of the admixture of
undersaturated air.

3.2 The Experiments

The appratus devised for the experiments is illustrated in Figure (3.1). Two moist air streams, of temperatures, T_A and T_B ($T_A > T_B$), were produced by drawing air through a pair of bubblers partially filled with water. A pair of centrifugal traps was then used to remove from these streams droplets produced by bubble bursting. The streams were subsequently mixed at the top of the fall tube, and since they were both almost saturated, a droplet cloud was formed by condensation. The flow rate of air through each bubbler, V_A and V_B, was measured using a flowmeter and could be varied electrically. Since the entire system was airtight the total flowrate through it was $V_A + V_B$.

The iron fall tube was cylindrical, of length 5m and diameter 0.25m. Its interior walls were lined with blotting paper. Plastic honeycombing was installed over the entire cross-sectional area of the tube, near its top and its base, in order to eliminate large-scale turbulence. This reduced the length of tube over which the spectral evolution could be studied to about 4m. The minimum total flowrate which could be employed, about 80 l min^{-1}, corresponded to a mean air speed U of about 40 mm s^{-1} down the tube and thus the development of the droplet spectrum could be observed over a time interval of up to 100 s. Since the largest droplets grown in the tube were of diameter 12μm it is reasonable to assume that their relative sedimention was negligible during their

3.iii

passage down the tube. Nine ports, spaced at 0.5m
intervals within the working section, were employed for
sampling the cloud droplets, which were collected on
glass slides coated with magnesium oxide. The collec-
tion efficiencies of the slides for droplets of the size
range investigated were determined in a series of subsidi-
ary studies. Temperatures were measured at various levels
within the fall tube.

The liquid water content within the cloud could be
measured using an impactor. Cloudy air was drawn into it
and passed through a rectangular nozzle. Droplets contained
in the air were deposited on a slide covered with blotting
paper which was subsequently weighed. The values of liquid
water content, C, obtained in this manner were self-
consistent, and in reasonable agreement, with those obtained
by integrating over the measured size distribution of the
droplets. The estimated uncertainty in the measured values
of C was ± 15%. It was not possible to make measurements
of C at the same time as sampling the droplets passing
down the fall tube. Fortunately, this deficiency was
not important since it was found that conditions at any
level within the tube remained essentially constant for
periods of up to 20 minutes.

The effect on the droplet spectrum of mixing in
undersaturated but humidified laboratory air could
be investigated by opening either one or two circular
orifices located at or between the level of ports 3 or 4,
(port 1 was the highest). The relative humidity of this
air was typically about 90%. The diameter of the orifices

was either 6 or 25 mm and the total flow rate through them (V_C) was ranged in different experiments, from 6 to 40 l min^{-1}. In some experiments saturated air at a temperature exceeding that of the descending cloud was introduced at a flow rate V_D through orifices located at the level of port 6.

A number of subsidiary experiments were performed in order to investigate the reproducibility and validity of the results. The homogeneity of the spectrum across the tube was tested at various levels by locating sampling slides at various positions between the centre and 30 mm from a wall. The constancy of the spectrum at a particular level and at different positions at this level was studied by sampling at intervals during the typical period of an experiment. In all cases no significant variations in size distribution were found. Analysis of the numbers and sizes of droplets collected at various locations on the slides showed that the distribution was quite uniform and that the general procedure, which was to count and size the droplets collected on a central region of area 0.6 mm^2 provided reliable spectral information.

A good example of the level of reproducibility attained in these experiments is provided by Figure (3.2) and its associated Table (3.1). In this particular experiment (run VI) no entrainment of laboratory air occurred and the liquid water content C was measured at three levels to be 0.16 $\pm$ 0.02 g m^{-3}.

TABLE 3.1: Values of mean droplet diameter $\bar{d}$ and spectral
dispersion α, for the spectra measured at all nine
ports in Run VI. No mixing.

$T_A = 30.5^\circ C$; $T_B = 18^\circ C$; $V_A = 65$ 1 min^{-1}; $V_B = 55$ 1 min^{-1}

PORT	1	2	3	4	5	6	7	8	9
$\bar{d}$ (μm)	7.2	7.5	7.7	7.9	7.5	8.0	8.2	7.9	7.6
α	0.14	0.14	0.13	0.14	0.15	0.13	0.13	0.13	0.14

The histograms and tables show that although there are con-
siderable variations, from port to port, in the number of
droplets located within a particular size band, of width
1 μm, there is reasonable constancy in the values of the
overall spectral parameters $\bar{d}$, the mean droplet diameter,
and α, the measured dispersion. These parameters are defined
by the equations

$$\bar{d} = \sum_i N_i d_i / N \qquad (3.1)$$

$$\alpha = (\sum N_i (d_i - \bar{d})^2)^{\frac{1}{2}} / N^{\frac{1}{2}} \bar{d} \qquad (3.2)$$

where N_i is the number of droplets per unit volume in the
ith size category; these have a diameter d_i. $N(= \sum_i N_i)$ is the
total drop concentration. The histograms also reveal the
absence of systematic variations in the values of N. This
finding, together with the observed approximate constancy
of water content C suggest that the loss of droplets by
deposition on the walls was negligible. This conclusion
was confirmed in other experiments. The Mean value of N

for the spectra presented in Figure (3.2) was 1300 cm^{-3}, and the standard deviation was $\pm$ 10%. This level of uncertainty was typical of those obtained in the other experiments.

3.3 Results

In all the acceptable experimental runs in which environmental air was not introduced into the descending cloud the mature spectrum was established by the time it reached port 2, and thereafter remained essentially unchanged. The dispersion α of the established spectra ranged from 0.13 to 0.16, the higher values being associated with larger values of N and C.

Table (3.2) presents measured values of N, $\bar{d}$, α and C for the experimental run VIII, in which undersaturated laboratory air was drawn in to the descending cloud at a rate of 6 l min^{-1} through a hole of diameter 6 mm located midway between ports 3 and 4. Table (3.2) is shown on the following page. The spectrum existing at port 2 is very similar in its properties to those obtained in the runs with no mixing, illustrated in Figure (3.2). The spectrum at port 3 is probably a consequence of partial dilution by the undersaturated stream, and is not useful. However, the spectra at ports, 4, 5, 6 and 7 are similar in their values of C and α, suggesting that the effects of the mixing process are largly complete at port 4 and then remain roughly constant up to port 7. The values of the measured dispersion α for ports 4 and 7 are more-or-less equal to that at port 2, although the liquid water content has dropped to almost half its former value. In the final

Table 3.2: Values of total droplet concentration N, water content C_ℓ, mean droplet diameter $\bar{d}$, and dispersion α for the spectra measured at all nine ports in the mixing experiment VIII. $T_A = 27^{\circ}C$; $T_B = 19.5^{\circ}C$; $V_A = 60 \ 1 \ min^{-1}$; $V_B = 62.5 \ 1 \ min^{-1}$; $V_C = 6 \ 1 \ min^{-1}$.

PORT	1	2	3	4	5	6	7	8	9
N (cm^{-3})	760	840	650	410	440	390	340	560	530
C_ℓ (g m^{-3})	0.16	0.19	0.14	0.10	0.10	0.11	0.09	0.14	0.16
$\bar{d}$ (μm)	7.2	7.3	7.4	7.6	7.4	7.8	7.9	8.1	8.1
α	0.14	0.14	0.12	0.15	0.16	0.15	0.14	0.18	0.18

stages of its journey through the fall-tube some growth of the spectrum occurs, presumably as a consequence of the observed cooling of the descending cloud. The mean size, water content and the dispersion of the spectrum all increase between ports 7 and 9. If we compare the spectra at ports 2 and 9 we see that the overall effect of mixing in of dry air followed by some regrowth of the spectrum is to decrease C by 16%, to decrease N by 37%, to increase $\bar{d}$ by 10% and to increase α by 19%.

It is perhaps appropriate to stress at this point that α is the <u>measured</u> dispersion. Although condensational growth of a complete spectrum will always, in the absence of other factors, act to decrease the dispersion, it is necessary to take account of the fact, in our experiments, that droplets of diameter less than 6 μm could not be detected. The recorded increase in α and N when **regrowth** occurs, is a consequence of the growth to detectable size, of droplets smaller than 6μm in diameter.

The most significant finding, which was confirmed in the other mixing experiments of this type - irrespective of the size of orifice through which the undersaturated air was introduced - was that α is essentially unaffected by the mixing, even though C is substantially reduced. This finding may be illustrated by comparing the spectra for ports 2 and 4 of run VIII displayed in the upper row of figure (3.3). It is seen that droplets are removed in almost equal proportions from all size categories, and the shape of the spectrum is preserved. There is some preferential removal of smaller droplets, as evinced

by the slight decrease of $\bar{d}$, but the effect is minor.

Confirmation of the generality of this result in these experiments is provided by the spectra presented in the lower row of Figure (3.3) and ports 2, 4 and 7 in run XIX. In this experiment undersaturated air was introduced at port 3 and saturated air, at a temperature in excess of that in the cloud at the same level, at port 6. The spectral properties measured at each port are presented in Table (3.3).

Table 3.3: Values of total droplet concentration N, water content C, mean droplet diameter $\bar{d}$ and dispersion α for the spectra measured at all sampling ports employed in the mixing experiment XIX.
$T_A=39^\circ C$; $T_B=19^\circ C$; $V_A=120$ l min^{-1}; $V_B=150$ l min^{-1}; $V_C=25$ l min^{-1}; $V_D=80$ l min^{-1}.

PORT	1	2	4	5	7	8	9
N (cm-3)	2500	2550	1500	1350	1900	1800	1850
C (g m-3)	0.64	0.67	0.35	0.29	0.56	0.56	0.49
$\bar{d}$ (um)	7.7	7.7	7.5	7.3	7.9	8.1	7,7
α	0.17	0.17	0.16	0.15	0.21	0.20	0.20

It is seen, as with run VIII, that there are three readily distinguishable regimes. At port 2, where no mixing has occurred, the established cloud possesses a liquid water content of 0.67 g m^{-3} and the measured dispersion α is 0.17. Between ports 3 and 6 it is found that the admixture of

of undersaturated air has resulted in C falling to about
half of its original value with α and $\bar{d}$ being only marginally
changed. The saturated air introduced at port 6 causes
regrowth of the droplet population, and C rises to $0.56g\ m^{-3}$.
The mean diameter $\bar{d}$ increases and the dispersion is
increased to about 0.20. Thus we obtain a similar result
to that of run VIII - the overall effect of the mixing
process is to decrease C by about 16% and to increase α
by about 18%.

Some simple calculations were performed in order to
see how mixing might produce the spectral modifications
observed in run VIII. Specifically, the objective was to
determine how the spectrum measured at port 2 could evolve -
as a consequence of mixing- into that observed at port 4;
and also to see if regrowth of this spectrum could explain
that observed at port 9. Various spectra and spectral
properties pertaining to these calculations are presented
in Table 3.4

Table 3.4: Measured and calculated values of observable droplet concentrations N_i, total observable droplet concentration N, water content C, mean droplet diameter $\bar{d}$, and dispersion α, for spectra at ports 2, 4, and 9 in the mixing experiment VIII.

Spectrum A – measured at port 2; Spectrum B – uniform dilution of A to take account of mixing but not evaporation; Spectrum C – Measured at port 4; Spectrum D – calculated for Port 4 on basis of homogeneous mixing; Spectrum E – Calculations for Port 4 on basis of inhomogeneous mixing without partial evaporation; Spectrum F – Calculated for Port 4 on basis of inhomogeneous mixing with partial evaporation; Spectrum G – Measured at port 9; Spectrum H – Calculated for port 9 from growth of Spectrum F.

Note that the droplet d < 6um present in Spectrum F are not included in the table, since they could not be observed in the experiments.

SPECTRUM	N_i (cm^{-3}) d(μm)								N (cm^{-3})	$\bar{d}$ (μm)	C (g m^{-3})	α
	6	7	8	9	10	11	12	13				
A	194	312	228	74	30	0	2	0	840	7.3	0.19	0.145
B	184	297	218	70	29	0	2	0	800	7.3	0.18	0.145
C	45	184	110	47	22	6	1	0	414	7.6	0.10	0.146
D	296	217	70	29	0	2	0	0	614	6.7	0.10	0.128
E	98	156	114	37	15	0	1	0	454	7.3	0.10	0.145
F	78	125	144	47	19	0	1	0	414	7.5	0.10	0.145
G	42	190	129	75	61	18	8	5	527	8.1	0.16	0.178
H	113	78	125	144	47	19	0	1	527	8.0	0.16	0.178

As a consequence of introducing air of relative humidity about 90% at a rate of 6 l min^{-1} into the descending cloud, of flowrate 122 l min^{-1}, the liquid water

content is reduced from 0.19 g m^{-3} at port 2 (Spectrum A in Table (3.4) to 0.10 g m^{-3} at port 4 (Spectrum C). On the classical model of mixing, employed by Warner, Mason and Jonas, and others the number of droplets per unit volume will be reduced by the fraction 6/122, which causes N to fall from 840 cm^{-3} to 800 cm^{-3} – yielding Spectrum B – and these remaining droplets will then evaporate in an environment of uniform undersaturation. Although not strictly correct, the form of the evaporation equation used by Warner (1969b) is sufficiently precise for our purposes, and was therefore employed. In fact some simplification is possible because the curvature and solubility terms may be neglected to a first order approximation for $d \geq 6$ μm. The evaporation equation at $t = 0$ may thus be written

$$(r + a) \, dr/dt = 1.35 \, S_o \qquad (3.3)$$

where S_o (=0.35%) is the undersaturation which, when exhausted, will reduce C from 0.19 to 0.10 g m^{-3}. In this equation, which is appropriate for our measured temperature of 24°C, r and characteristic length a related to the condensation coefficient are in micrometres. a was taken to be 5μm, but the precise choice is not critical. If Spectrum B is allowed to evaporate, according to the equation (3.3), with S_o replaced by the (increasing) value of S, until the relative humidity in the cloud has risen to 100% the spectrum D is produced. We see that it is very different from the Spectrum C actually observed at port 4. The calculated value of N is much larger and of $\bar{d}$ and α much smaller thant the corresponding measured values, and we conclude that the modifications to the spectra

are inexplicable in terms of homogeneous mixing.

The crudest possible description of spectral modification produced by inhomogeneous mixing would be to propose a process whereby the mixed airmass consists of small regions in which admixture of the dry environmental air has resulted in complete evaporation of all the droplets, interspersed with small regions to which very little dry air has been added. The average properties of such a mixture would closely resemble what we observe ie a reduction of the total count N and of the liquid water content C but no change in the mean drop diameter $\bar{d}$ nor in the dispersion α. If we assume that in the regions to which just a little dry air has been added some droplet evaporation occurs, affecting primarily the smaller droplets, we would expect the average properties of the mixed airmass to have a slight reduction in N and increase in $\bar{d}$ compared to the original values, a prediction which is in close agreement with our observed results.

As a rough illustration of this description of the role of mixing on the drop spectrum - complete evaporation of some drops from all size categories, combined with some preferential evaporation of the smaller ones - we note the observations N = 414 cm^{-3} at port 4 and N = 527 cm^{-3} in the regrown spectrum at port 9. Thus we assume that in addition to the spectrum observed at port 4 there were 113 cm^{-3} droplets below the detectable size limit. If, to take account of preferential evaporation, we arbitrarily assume that these unobservable drops were of diameter 4.0μm, and had been removed in equal proportions from the two lowest size catagories (d = 6, 7μm) we derive Spectrum F

displayed in Table (3.4). This is seen to be in close agreement with that observed (Spectrum C). Finally, if we now allow Spectrum F, including the unobservable drops, to grow according to equation (3.3) until C has risen to 0.16 g m^{-3} (and N to 527 cm^{-3}) Spectrum H is produced. Its values of α and $\bar{d}$ are seen to agree well with those of Spectrum G, observed at port 9.

It would be completely unjustifiable to conclude that these calculations - or the rudimentary description of the role of mixing on which they are based - have much quantitative significance. However, it would appear safe to contend that the spectral modification observed are quite inexplicable in terms of homogeneous mixing but are consistent with an inhomogeneous process in which some drops of all sizes are completely evaporated, and some overall evaporation of the spectrum also occurs.

3.4 Discussion

As mentioned earlier, Warner (1969b) has shown that the dispersion of the droplet spectra in cumulus clouds at levels of up to about 200 m is explicable when account is taken of the reduced rates of diffusional growth associated with values of condensation coefficient substantially below unity. However, the shape and dispersion of droplet spectra at higher levels requires the operation of an additional process. Entrainment of undersaturated environmental air is clearly the most likely candidate since it produces both the sub-adiabatic cloud water concentrations and - by activation of fresh nuclei - the continued presence of small droplets. However, as previously discussed, Warner (1973a)

concludes from his calculations that a simple mixing pro-
cess is unimportant in determining the drop size distri-
bution. Warner (1975) is also unable to accept the multi-
thermal model of droplet evolution presented by Mason
and Jonas (1974) and Jonas and Mason (1975).

It is recognised that the mixing experiments described
in Section (3.3) were crude and in essential respects
unrepresentative of entrainment within natural clouds.
Nevertheless, it is possible that they focus attention upon
one important feature of the mixing process - its inhomo-
geneity. The calculations of the cited workers have all
been based on the assumption that the mixing is uniform and
homogeneous. In other words, they assume that apart from
the drops which are present in the cloudy air replaced by
undersaturated air, all droplets at a given level in the
cloud are, at any time, exposed to identical conditions
of supersaturation or undersaturation. Thus it follows
that as they spectrum evolves - and the liquid water content
increase - as a consequence of the overall upward motion
of the cloud air the homogeneous mixing process envisaged
by Warner (1973a) will produce a spectrum consisting of
a gradually narrowing peak at the large-diameter and
followed by a plateau resulting from the continual
activation of fresh nuclei. Such an evolution was c
calculated by Warner, and discarded by him as being
inconsistent with the observational evidence.

However, in the present experiments the mixing has been shown to be far from homogeneous. Some droplets are removed, by evaporation, from all size categories and - to judge from the measured spectra and observed approximate constancy of the dispersion - many other droplets are negligibly affected by the mixing process.

Although it would be unjustifiable to use our experimental results to attempt a quantitative treatment of the effect of inhomogeneous mixing on spectral evolution, some general predictions may be made. The spectra observed near cloud base have been shown by Warner (1969b) to be explicable in terms of condensational growth without the intervention of mixing. We now consider inhomogeneous mixing of this cloud air with its environment as it rises. We assume that the mixing occurs in the manner described in Section (3.3) ie some droplets are removed from all size categories and there is also some preferential evaporation of the smaller droplets. In addition, following earlier workers, we invoke the activation of fresh nuclei drawn into the cloud by the mixing process. In this situation the original, large diameter peak will not narrow as the cloudy air ascends since some droplets within it will be scarcely affected by the mixing process, while the growth of others - particularly the smaller ones - will be

significantly inhibited. Thus, as the cloud ascends, the large diameter peak will broaden and gradually lose its identity. This general pattern of evolution was commonly observed by Warner.

Knollenberg (1976) has presented a pair of droplet spectra measured a few metres apart near cloud base which appear to lend support to the arguments presented herein. The mode diameter is more or less constant but one spectrum contains more than twice as many droplets that the other. He states (private communication) that such inhomogeneities are often foud.

It should be stressed, however, that this simple model of inhomogeneous mixing has no quantitative support. Indeed it is not susceptible to realistic quantitative test until more information exists on the nature of the mixing process - on all scales - within cumulus clouds. For example, the simple ideas presented in this section do not appear able to explain the bimodal spectra frequently (but not generally) observed by Warner.

An equivalent description of inhomogeneous mixing can be presented in terms of <u>fluotuations in supersaturation not tied to fluctuations in vertical air velocity.</u> Bartlett (1968) performed some calculations yielding the conclusion that fluctuations in supersaturation resulting from turbulent variations in updraught velocity do not have a crucial effect upon spectral breadth. Essentially, this is because the increase in size of a droplet as it rises between two levels is insensitive to the speed with which it makes the journey - slower growth over a longer time

in a lower supersaturation (velocity) air parcel just about balancing faster growth over a shorter time in a higher velocity updraught. However, if inhomogeneities in super-saturation are produced by the entrainment of environ-mental air - as the present experiments suggest - spectral broadening can occur because the velocity/supersaturation relationship is not perfectly reversible.

3.xviii

4. ELECTRICAL STUDIES OF TURBULENT MIXING OF AEROSOL TRAPPED AT AN INVERSION

4.1 Introduction

The role of eddy diffusion in atmospheric transport processes is known to be of great importance, but an accurate quantitative theory is not available at present. This is largely a consequence of the difficulty involved in making the required comprehensive direct and reliable measurements. Accordingly, it is appropriate to explore unconventional and seemingly indirect techniques for studying eddy diffusion.

We describe an electrical technique for exploring eddy diffusive mixing in the vicinity of a temperature inversion. In essence, it consists of measuring simultaneously the vertical electric field, E, and the ionic conductivity λ of the atmosphere - which may be subdivided into positive and negative components, λ_+ and λ_-. Values of eddy diffusivity above and below the inversions, k_1 and k_2 respectively, may be determined by examination of the vertical profiles of E and λ.

The feasibility of such an approach became evident when research flights in the Meteorological Office Varsity aircraft revealed that the sharp decrease in λ just below an inversion - as a consequence of ionic immobilisation on trapped aerosol particles - was not accompanied by a correspondingly sharp increase in E. The electric field increased much more slowly with increasing distance

4.i

below the inversion and its profile was in good agreement with that of dewpoint. These observations, which are described in detail later are indicative of the diffusion of spcae charge, originally created in the region of conductivity variation, into deeper layers of the atmosphere. Much weaker evidence was found for a smaller but qualitatively similar mixing process upwards through the inversion.

4.2 Theoretical Treatment

We consider a temperature inversion separating an upper region of the atmosphere of low aerosol content and high electrical conductivity λ_2, and a lower region of high aerosol content. Ions moving downwards through the inversion become trapped and relatively immobilised on aerosol particles and the conductivity λ will decrease. For simplicity, we assume that λ decreases linearly over a depth Z_1 until a lower constant value λ_1, is achieved. This assumption is well supported by our experimental findings. If no mixing processes occur then conservation of ionic air-earth current λE demands that E, has a constant value, E_2, above the inversion, increases throughout the layer of decreasing λ, and possesses a constant value, E_1 lower down; $\lambda E (=\lambda_1 E_1 = \lambda_2 E_2)$ will be constant at all levels.

However, let us now suppose that mixing occurs between these three regions, as a consequence of eddy diffusion. Specifically, we consider the transport of space charge, of density ρ, created in the region of conductivity gradient, and characterise this eddy diffusion in these regions

by the diffusion constants K_2, K and K_1. Charge transported upwards through the inversion will constitute a current moving in opposition to the ionic flow, while that moving downwards through the lower boundary will reinforce the ionic current. Since, in equilibrium, the total air-earth current J must be conserved at all levels the existence of this imagined mixing process will cause an increase in λE around the top of this middle layer, and a decrease around the bottom. It is also to be expected that since the vertical extension of the field gradient, resulting from the transport of space-charge from this layer, depends upon the efficiency of the mixing process, it should be possible to determine values of the diffusion coefficients from the observed structure of E. This possibility will now be investigated mathematically.

At each interface E and ρ must be continuous and satisfy the equations

$$J = \lambda E + k\frac{d\rho}{dz} \qquad (4.1)$$

and

$$\frac{dE}{dz} = \frac{-\rho}{\epsilon_0} \qquad (4.2)$$

where ϵ_0 is the permittivity of free space. These two equations may be combined to give

$$J = \lambda E - \epsilon_0 K\frac{d^2E}{dz^2} \qquad (4.3)$$

The form of solution of equation (4.3) and the method for establishing values of K_1 and K_2 will first be illustrated by considering a limiting case in which the charge in λ is discontinuous at z=0 (ie $z_1 = 0$, $d\lambda/dz = \infty$).

4.iii

In these circumstances the solutions for E and ρ are:

for $z < 0$ (above the discontinuity)

$$E = \frac{J}{\lambda_2}\left[1 + \frac{(\frac{\lambda_2}{\lambda_1} - 1)\, e^{n_2 z}}{(1 + \sqrt{\frac{\lambda_2 K_1}{\lambda_1 K_2}})}\right]$$

$$\rho = -\frac{J}{\lambda_2}\left[\frac{(\frac{\lambda_2}{\lambda_1} - 1)\,\epsilon_0 n_2 e^{n_2 z}}{(1 + \sqrt{\frac{\lambda_2 K_1}{\lambda_1 K_2}})}\right]$$

where $\quad n_2^2 = \dfrac{\lambda_2}{\epsilon_0 K_2}$

and for $z > 0$ (below the discontinuity)

$$E = \frac{J}{\lambda_1}\left[1 + \frac{(\frac{\lambda_1}{\lambda_2} - 1)\, e^{-n_1 z}}{(1 + \sqrt{\frac{\lambda_1 K_2}{\lambda_2 K_1}})}\right]$$

$$\rho = \frac{J}{\lambda_1}\,\frac{\epsilon_0 n_1\,(\frac{\lambda_1}{\lambda_2} - 1)\, e^{-n_1 z}}{(1 + \sqrt{\frac{\lambda_1 K_2}{\lambda_2 K_1}})}$$

where $\quad n_1^2 = \dfrac{\lambda_1}{\epsilon_0 K_2}$

4.iv

These expressions for E and ρ satisfy the equations (4.2) and (4.3) and give E, ρ (and hence dE/dz) continuous at $z = 0$, where

$$E = J \left\{ \frac{\sqrt{K_2/\lambda_1} + \sqrt{K_1/\lambda_2}}{\sqrt{\lambda_2 K_1} + \sqrt{\lambda_1 K_2}} \right\}$$

and

$$\rho = J \left\{ \frac{\sqrt{\varepsilon_0 \lambda_1/\lambda_2} - \sqrt{\varepsilon_0 \lambda_2/\lambda_1}}{\sqrt{\lambda_1 K_1} + \sqrt{\lambda_2 K_2}} \right\}$$

It is seen from the solutions that determination of K_1 involves simply a determination of the exponent of n_1 by curve fitting below the discontinuity, and a knowledge of the constant conductivity λ_1. An identical procedure can be followed to determine the eddy diffusion coefficient above the inversion, K_2.

Having established in principle, the feasibility of determining K_1 and K_2 from measurements of E and λ_1, we now consider the more realistic situation, illustrated in figure (4.1), in which the region of changing conductivity is of finite depth Z_1. We assume the conductivity gradient in this region to be constant, and the governing equation becomes, for $0 < z < Z_1$,

$$J = \left\{ \lambda_2 + \frac{z}{Z_1}(\lambda_1 - \lambda_2) \right\} E - \varepsilon_0 K \frac{d^2 E}{dz^2} \qquad (4.4)$$

Exact solutions to equation (4.4) have been obtained computationally. However, a simple analytic solution is

4.v

available in the case where Z_1 is small compared with the characteristic length describing the vertical distance over which E changes. In this case we may assume that the two terms contributing predominantly to J, which must be preserved, are $d\lambda/dz$ – which is taken to be constant – and $\varepsilon_o K d^2 E/dz^2$. In this circumstance equation (4.4) becomes

$$J = \lambda \varepsilon_o - \varepsilon_o K \frac{d^2 E}{dz^2} \tag{4.5}$$

where $\lambda = \lambda_2 + (\lambda_1 - \lambda_2)(z/Z_1)$.

The solutions of equations (4.3) and (4.5) are

$z < 0,$
$$E = \frac{J}{\lambda_2} + Be^{n_2 z} \tag{4.6}$$

where $n_2^2 = \frac{\lambda_2}{\varepsilon_o K_2}$

$0 < z < Z_1,$

$$E = \frac{J}{\varepsilon_o K} \cdot \frac{z^2}{2} + E_o \{1 + \frac{\lambda_2 z^2}{} + \frac{(\lambda_1 - \lambda_2) z^2}{}\} + Cz, \tag{4.7}$$

$z > Z_1$

$$E = \frac{J}{\lambda_1} + Ae^{-n_1(z - Z_1)} \tag{4.8}$$

where $n_1 = \frac{\lambda_1}{\varepsilon_o K_1}$

The constants A, B, C and E_o may be determined from the conditions that E and dE/dz are continuous at $z = 0, Z_1$ and we find

$$-An_1 = -\frac{JZ_1}{\varepsilon_o K} + \frac{E_o Z_1}{2\varepsilon_o K} (\lambda_1 + \lambda_2) + C$$

$$B = C/n_2$$

$$C = n_2 (E_o - J/\lambda_2)$$

4.vi

and

$$E_0 = \frac{J[\frac{n_1}{\lambda_1} + \frac{n_2}{\lambda_2}(1+Z_1 n_1) + \frac{Z_1}{\epsilon_0 K}(1 + 0.5 n_1 Z_1)]}{n_1 + n_2(1+Z_1 n_1) + \frac{Z_1}{\epsilon_0 K}\{\lambda_1(\frac{1}{2} + Z_1 n_1) + \lambda_2(\frac{1}{2} + \frac{1}{3}Z_1 n_1)\}}$$

This treatment, in common with the exact solution, and
that presented earlier for the infinitely thin layer,
predicts exponentially varying fields E outside of the
layer of varying conductivity. Thus, curve fitting pro-
cedures may be employed to determine the exponents n_1
and n_2, and therefore, through equations (4.8) and (4.6),
values of K_1 and K_2. The application of this procedure
to the analysis of the structures of E and λ measured
during flights through temperature inversions is now
described cursorily. .

4.3 Field Studies

The field measurements were made using the Meteorological
Office Varsity aircraft, which carried: a cylindrical
field-mill, of the type devised by Kasemir, which measured
the vertical electric field E, and one horizontal comp-
onent; Gerdian tubes, modified for airplane usage, to
measure the positive and negative polar ionic conductivities,
λ_+ and λ_- respectively ($\lambda = \lambda_+ + \lambda_-$); a Cambridge hygro-
meter for measurement of the dew or frost point, T_D;
a Rosemount thermometer to record the air temperature, T;
and an accelerometer. In addition measurements were made
of air speed, pressure altitude, vertical velocity,
heading, ground-speed and drift. All of these parameters
were recorded on two $3\frac{1}{2}$" strip-chart recorders. The

electrical parameters were also recorded in digital form
on magnetic tape, in order to facilitate subsequent data
processing. All three recorders were synchronised by
means of a digital clock.

The accuracy of the measurements of E was estimated
to be $\pm$ 10%, or 5 V m^{-1}, whichever was greater, and changes
in E were detectable to $\pm$ 1%. In the case of the ionic
conductivity the absolute accuracy of the measurements
was estimated to be $\pm$ 15%. However, changes in conduc-
tivity of 10^{-15} Ω^{-1}m^{-1} could easily be detected. The
response times of the field mill and the conductivity
tubes were made equal and set at one second.

The general flight procedure consisted of a descent
to 500' followed by a slow (500' per minute) ascent to
determine the heights of any inversions. This was
followed by a series of "stepped race-tracks" such that
the major inversion was passed through, either in ascent
or descent on each of the straight legs of the race-track
at rates varying from 500 ft min^{-1} to 1500 ft min^{-1}.

A particularly clear cut and well documented set of
measurements was provided by the flight of 14 June 1975.
The weather over the UK was characterised by a surface
anticyclone of 1033 mb centred over the English Channel.
The associated upper ridge was discernable up to at least
100 mb, and led to a well marked inversion situated at
about 880 mb. The aircraft measurements were made over
the sea to the south of the Isle of Wight.

The air temperature and dewpoint recorded on the
initial climb from 500 ft is shown in Figure (4.2). The
top of the aerosol was well marked visually at about

3940 ft above sea level. This was confirmed by a reduction in turbulence sensed by the accelerometer at this height. The dewpoint lapse rate suggests that a layer of drier and presumably relatively pollution-free air existed at about 700 ft above sea level. The sea surface temperature at this time was approximately $13^{o}C$ so large scale convection is unlikely to have been present.

The raw data points from the field and conductivity measurements averaged over successive 10 second intervals are shown in Figure (4.1). The variations in E and λ follow those previously discussed, the vertical depth over which λ changes below the inversion being much less than that for E. Smoothed curves, corrected for a zero error in λ, are presented in Figure (4.3), which also displays the field-driven ionic current $E\lambda$. Although $E\lambda$ is more-or-less constant at large distances from the inversion it is seen to increase and then decrease, moving downwards through the discontinuity. This indicates that there is upward and downward mixing of charge originally trapped on the aerosol particles in the region of changing conductivity; the downward mixing being much more effective than the upward. The theoretical curves based on assumed diffusion lengths of 10 m above and 100 m below the inversion are in good agreement with those measurements.

This preliminary study will be extended, both theoretically and in the field, where it is planned to use the glider described in section 5.3 of this report.

5.   RECENT WORK AND FUTURE DEVELOPMENTS

5.1 Electrical Scavenging of Aerosols

Experiments are in preparation to investigate the
scavenging of submicrometre aerosol by electrified rain-
drops. Field studies have shown that even when the pre-
vailing electric fields are weak individual charges on
raindrops may be very substantial. This is because there
is often a mixture of positively and negatively charged
drops, resulting possibly from their collision and separa-
tion as they fall to ground in a rainshaft. Preliminary
evidence indicates that the capture efficiency is high,
even when the aerosol is uncharged. The experimental
plan for the first phase of these studies is to produce
an aerosol of known and narrow size-range in the band
0.1 to 5 µm by evaporating a population of larger drop-
lets of sodium chloride solution produced by a spinning-top
device. Drops of controlled charge and size will be
directed through this aerosol cloud and the collection
efficiency determined, for a wide range of parameters,
by measuring the amount of NaCl captured by the drops.

5.2 An Optical Scattering Nephelometer

A major instrumental development has been the design
and construction of a novel device for the measurement
of droplet size distributions in clouds. This work was
conducted in two stages. First, an instrument was built
and tested in laboratory clouds. Satisfactory performance
led to the construction, for field use, of a more versatile

5.1

and rugged version, which possesses the additional facility of direct measurement of water content and visibility within clouds.

The principle of this technique is to measure the intensity of the light scattered at a set of angles from a large number of droplets contained in the cloud - typically, a volume of 70 cm^{-3} is employed. A numerical inversion is then obtained of the integral equation describing the scattering pattern as a superposition of the individual patterns from all of the droplets within the scattering volume. A matrix is used to approximate the integral equation and an inversion is obtained using the method of least-squares.

A requirement of a successful device based on this principle is that the scattering patterns are sensitive to variations in droplet size. More precisely, the matrix of the scattering functions should be closely orthogonal. Accordingly, calculations were undertaken to determine the optimum set of scattering angles. These led to the choice of narrow angle forward scattering, which possesses the additional practical advantage of convenient and accurate measurement.

In essence, the instrument is an optical diffractometer with a horizontal axis, and is shown schematically in Figure 5.1. Illumination is provided by a three milliwatt helium-neon laser. The scattering pattern was measured using a novel technique. Fibre optic light guides were embedded in a metal disc in order to channel the light from the scattering pattern on to a photomultiplier.

When the disc is rotated, a rapid and repetitive scan
of the scattering pattern is obtained. The photomulti-
plier signal is amplified and then digitised. Finally,
this numerical data is treated on a computer, and the
droplet size distributions are presented in histogram form.

We now outline the extension of this principle leading
to a direct measurement of liquid water content. Calcula-
tions show that the sum of the intensities of the light
scattered by a droplet at specific angles have been identi-
fied which confirm this relationship to within ± 2% for
droplets of radius between 1 and 40 um. This finding
enables the liquid water content of the cloud to be measured
directly, continuously and accurately. On a similar
principle, another combination of scattering angles can
be selected such that the combined response is proportional
to the surface area of the droplets. This relationship
is found to hold, over the same size range, to within
± 6%. Thus the reciprocal of the measured signal may
be taken as an indicator of the visibility within the cloud.
These techniques for recording liquid water content and
visibility, in addition to droplet size distribution,
have been incorporated into the field-**version** of the
instrument, which has recnetly been built.

The fibre optic device for measuring droplet size
distributions has been tested within laboratory clouds.
The results agreed well, over a wide range of conditions,
with those obtained using the standard coated cylinder
techniques.

5.3 Airborne Experiments Using an Instrumented Sailplane

It is proposed to extend the scope of the aerosol studies being conducted at Great Dun Fell by utilising an instrumented sailplane which is capable of sustained soaring performance and is also built to withstand the severe turbulence which can be encountered in large convective clouds. The sailplane (Figure 5.2) has a wingspan of 15m, is designed to fly within clouds, and will be able to carry about 35 kg of instruments. Its flight speed can range from 60 to 250 km hr^{-1}, its minimum sinking speed in still air is 0.7 m sec^{-1} at 75 km hr^{-1}.

Topics to be investigated include: the measurement of cloud droplet spectra in cumulus and mountain lee-wave clouds, and the vertical structure of the atmospheric aerosol in the lower 3km of the boundary layer.

Sailplane measurements in the first topic would complement the existing ground based experiments at GDF since it would be possible to examine the growth and subsequent modification of droplet spectra in both cumulus and mountain wave clouds and relate these findings to other parameters such as liquid water content and height above cloud base. The vertical velocity of the air can be calculated from the equation of motion of the sailplane (Dye and Tootenhoofd, 1973). By centering the sailplane in the strongest part of the updraught, measurements can be made whilst climbing towards the top of the cloud.

The second topic is concerned with the relation between aerosol concentration profiles measured on the sailplane and various meteorological parameters including the

5.iv

stability of the layer and the degree of turbulent mixing.

A particularly worthwhile situation to examine is thought to be that of a layer of high aerosol concentration contained by a temperature inversion or hydrolapse. Airborne measurements have already been made of ion concentrations and vertical electrical field above and below temperature inversions and it has been found that the above-mentioned electrical parameters can be used to determine the degree of eddy diffusion occurring through the inversion. This has been described more fully in section4.

5.v

REFERENCES

Bartlett J T   1968   Proc Int Conf on Cloud Phys,
                                       Toronto, pp 515-517.

Dye J E & Tootenhoofd V 1973   VIII Conf on Severe Local
                                       Storms, Oct 15-17 1973,
                                       AMS, Boston, Mass.

Georgii HW   Wotzel G C 1970   JGR, 75, 1727-1732

Gormley P & Kennedy M 1949   Proc Roy Irish Acad, 52A, 163

Jaenicke R   1971   Staub-Reinhalt.Luft, 31, pp1-10

Jaenicke R & Blifford IH 1974   Aerosol Science, 5, pp 457-464.

Jonas P R & Mason B J   1974   Q J R Met Soc, 100, pp 286-295

Knollenberg R G   1976   Proc Int Conf Cloud Phys,
                                       Boulder, Colorado, pp 554-561.

Mason B J   1975   Q J Roy Met Soc, 101, 178-181

Mason B J & Jonas P R   1974   Q J R Met Soc, 100, 23-28

Metnieks A L &   1959   Geophys Bull, No 16, Dublin
Pollak L W   Institute for Advanced Studies.

Rich T A, Pollak L W &   1959   Geophysica Pure & Applicata,
Metnieks A L   Milano, 44, pp 233-241

Warner J   1969a J Atmos Sci, 26, 1049-1059

                         1969b J Atmos Sci, 26, 1272-1282

                         1970   J Atmos Sci, 27, 682-688

                         1973a J Atmos Sci, 30, 256-261

                         1973b J Atmos Sci, 30, 1724-1726

                         1975   Q J Roy Met Soc, 101, 176-181

<u>Figure 2.1</u>

UMIST FIELD RESEARCH STATION, GREAT DUN FELL,
CUMBRIA.
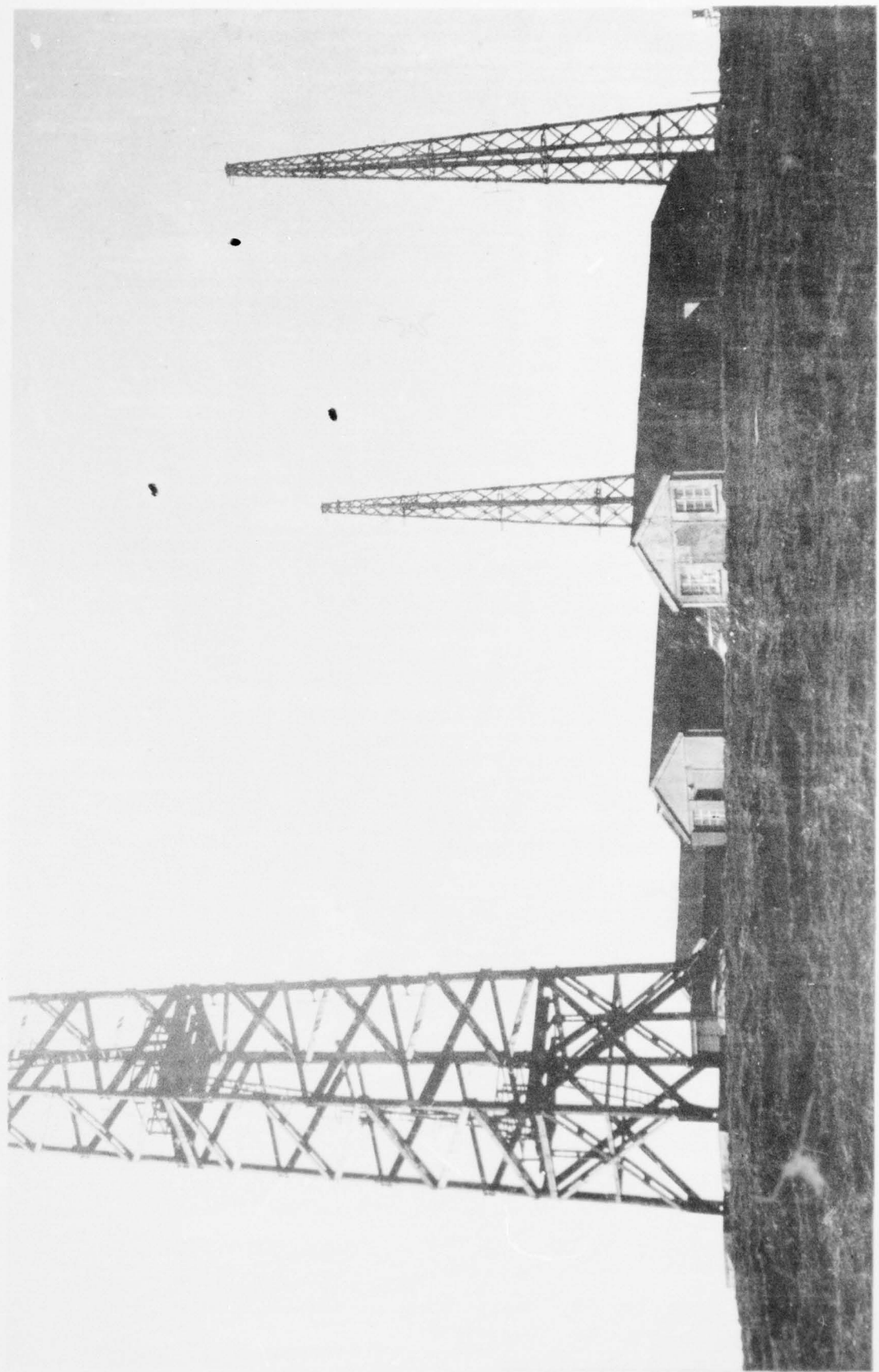
Figure 2.2

THE PHOTOELECTRIC NUCLEUS COUNTERS AND DOUBLE STAGE
IMPACTORS
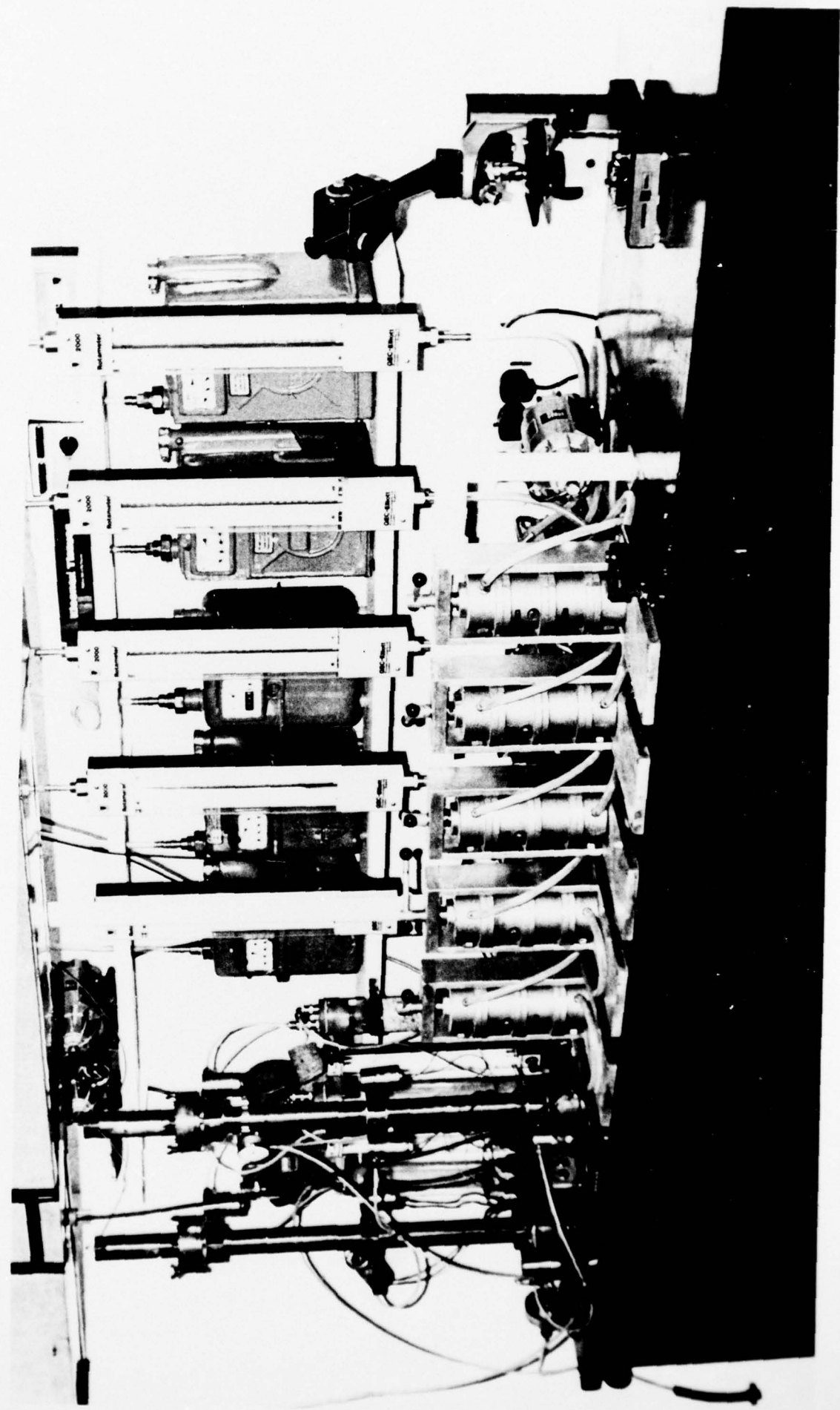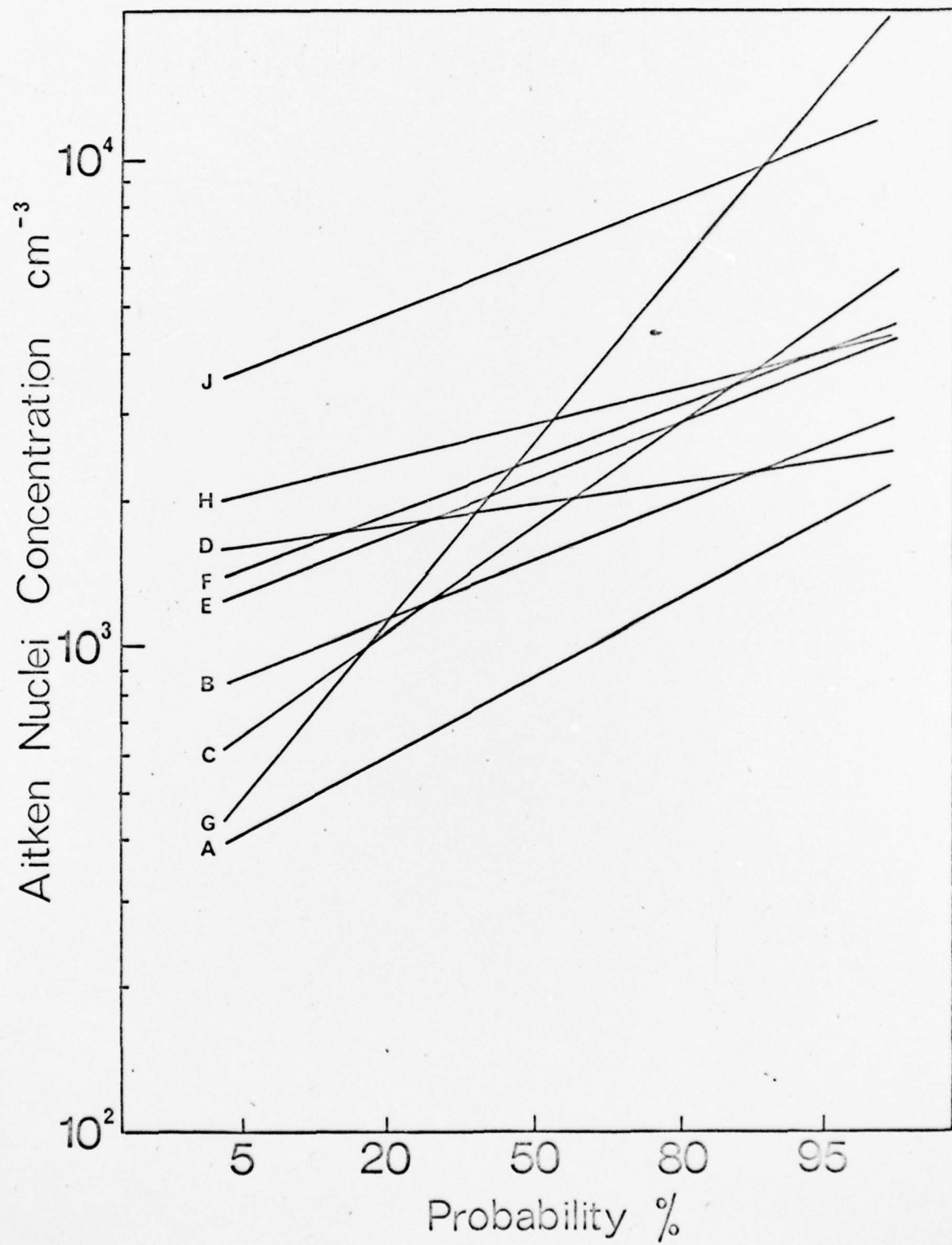
fig 2.3

BLOCK DIAGRAM OF KEILY PROBE/LWC SYSTEM

fig 2.4

Air in —[F]—[B]—[C]— Mixing Volume —[C]—[B]—[F]— Air in

Honeycomb

T_1 ——— P1

T_2 ——— P2

Air in —[F]—[B]—[C]— Mixing Volume —[C]—[B]—[F]— Air in

Honeycomb

T_1 ——— P1

T_2 ——— P2
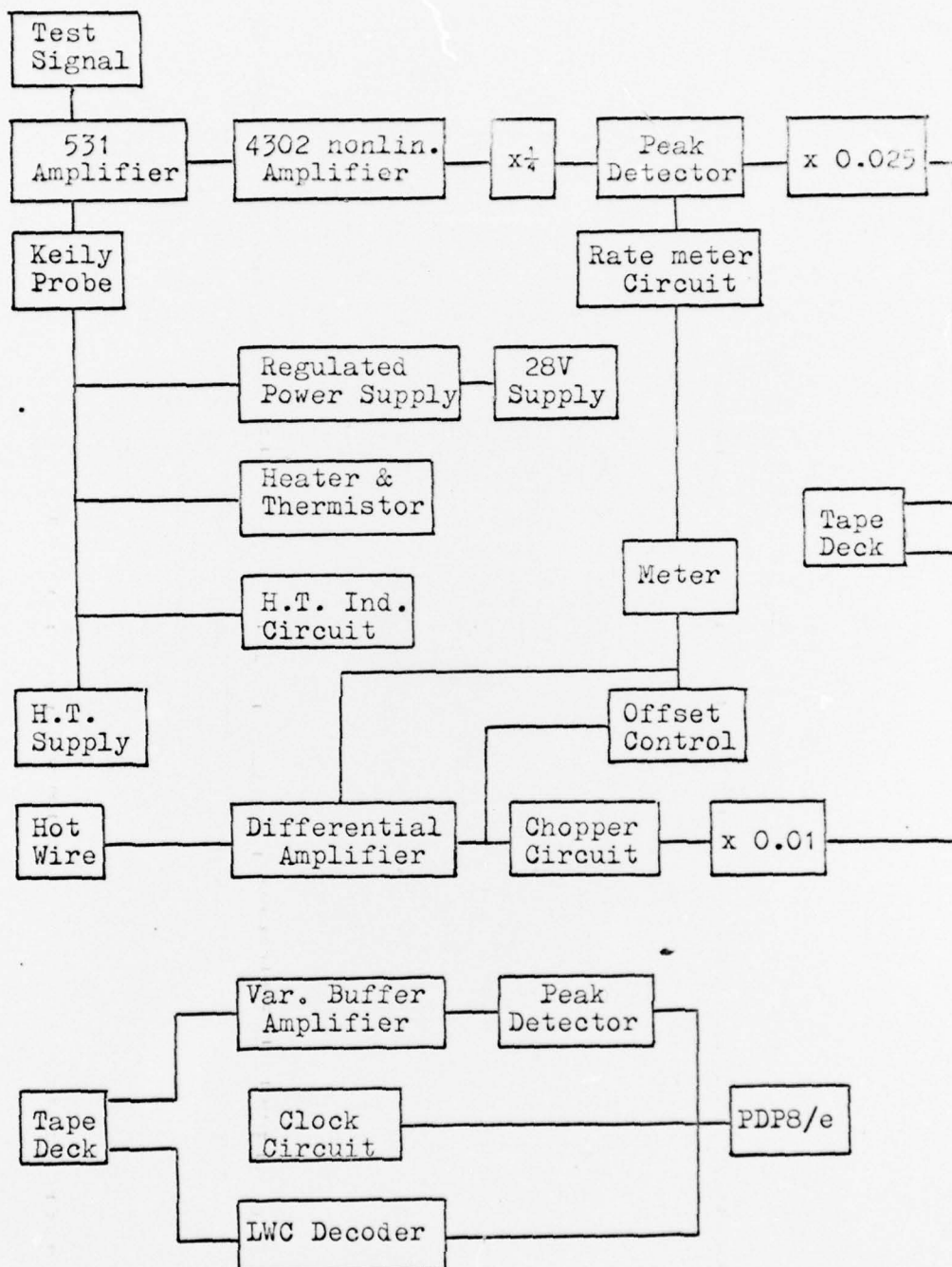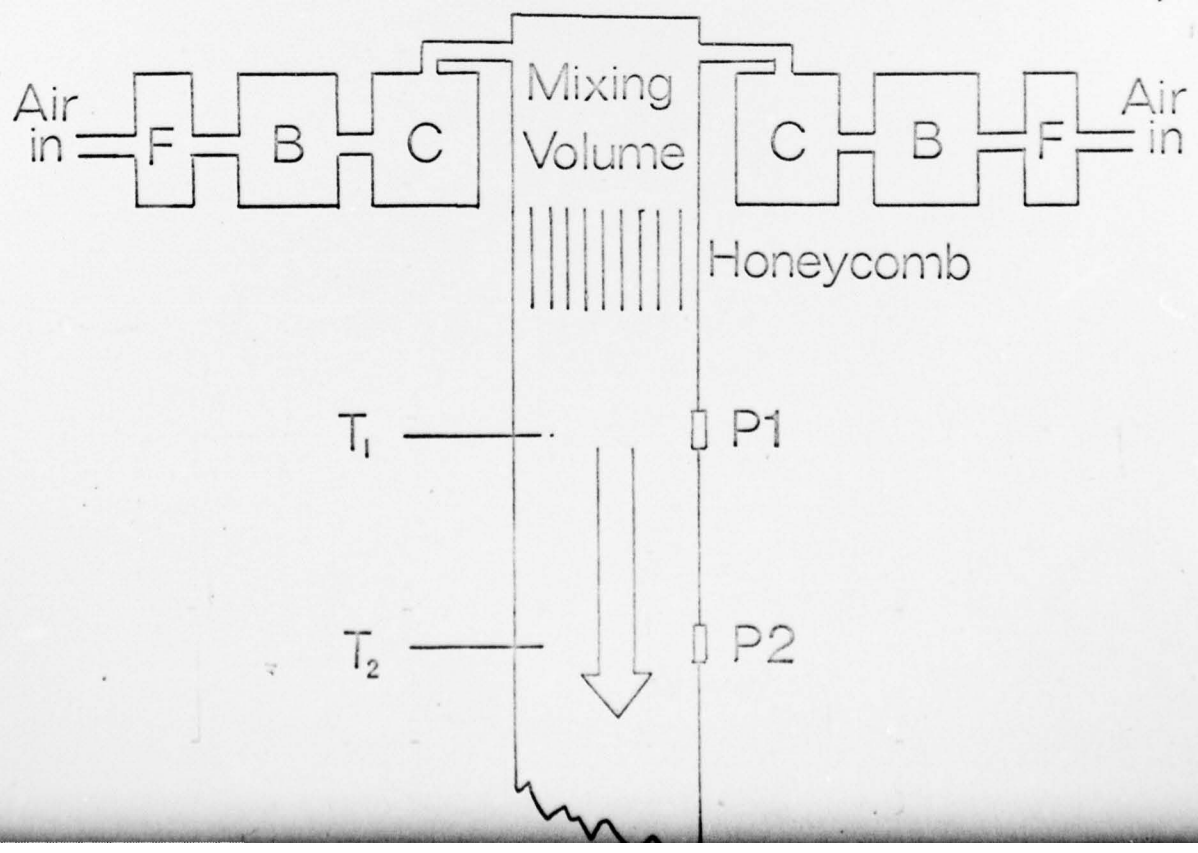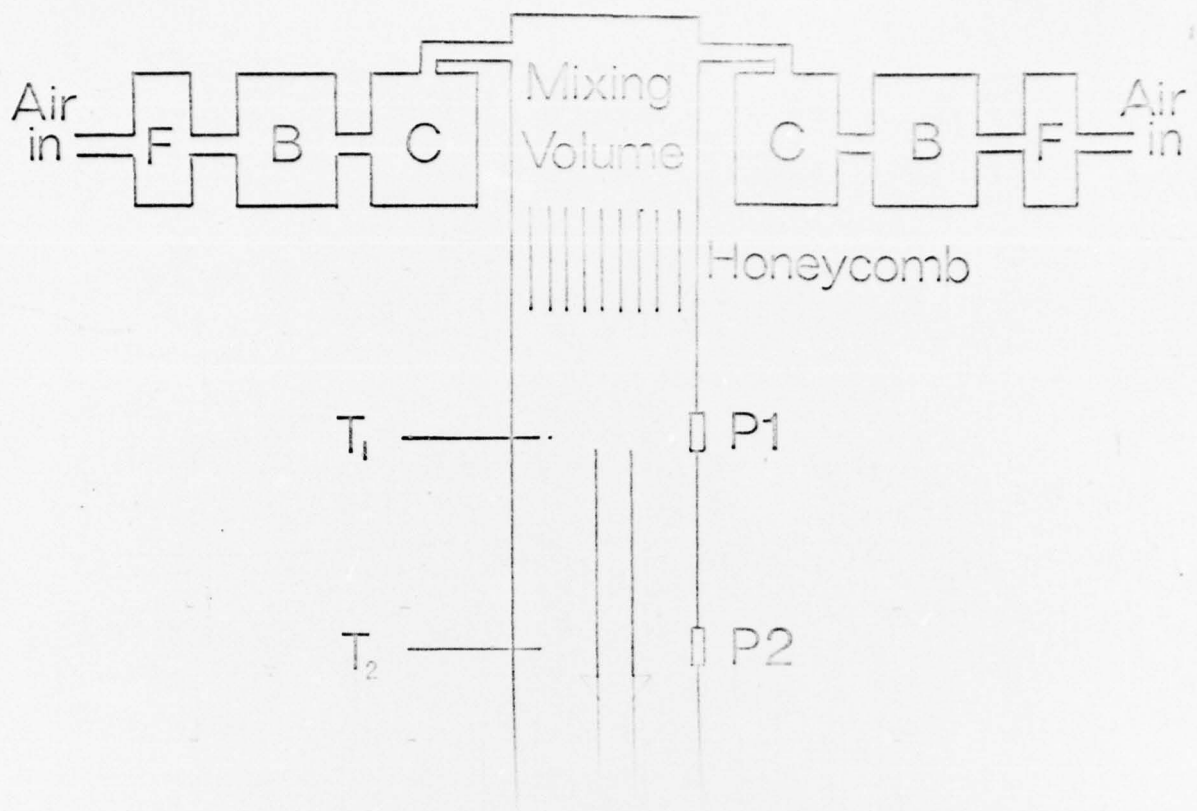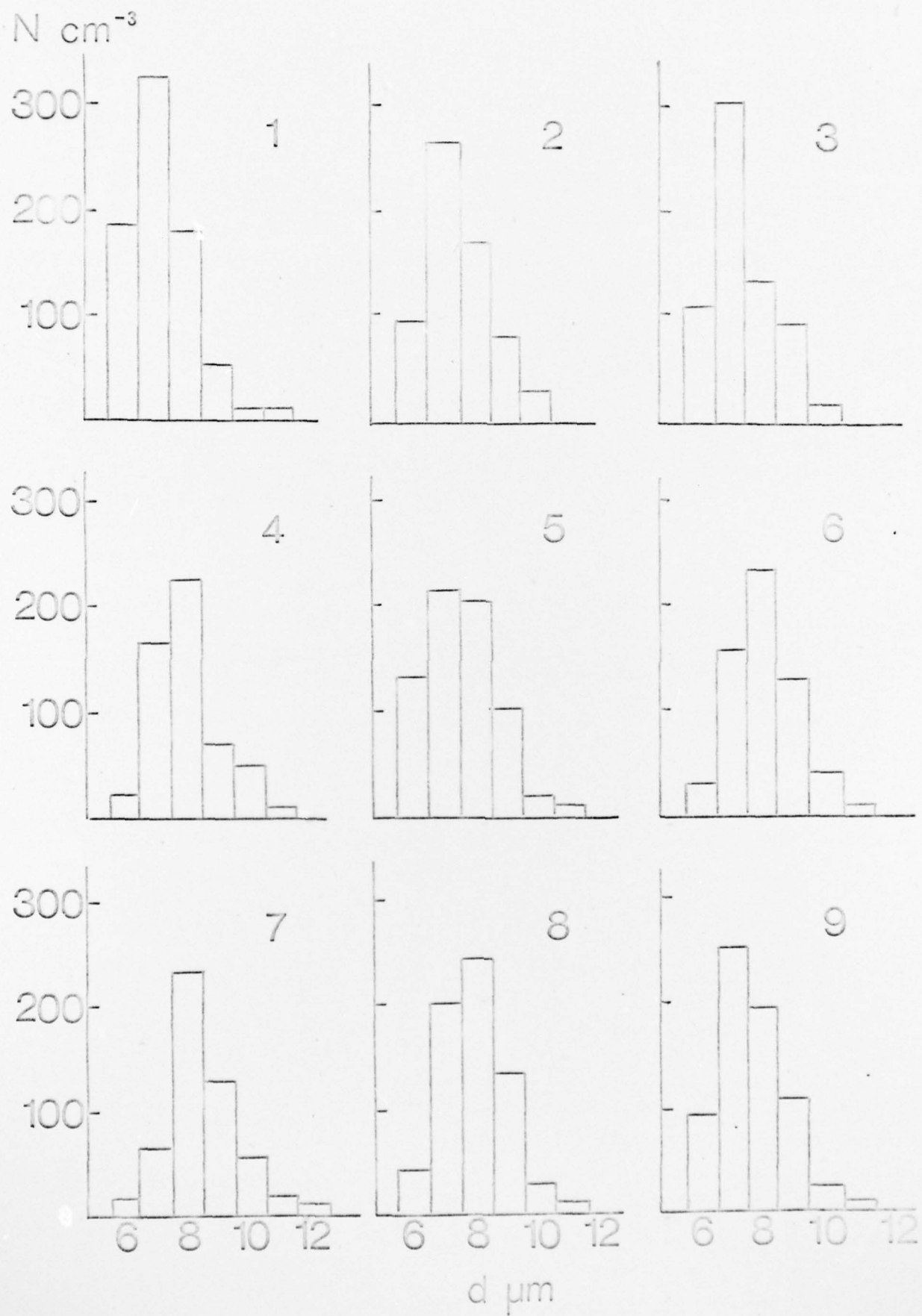
fig 3.2
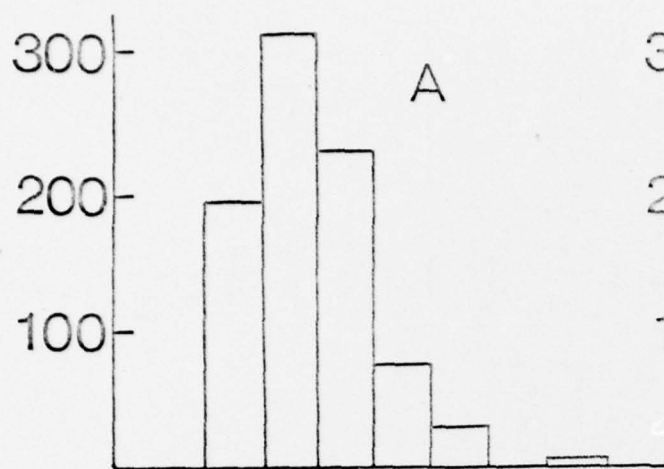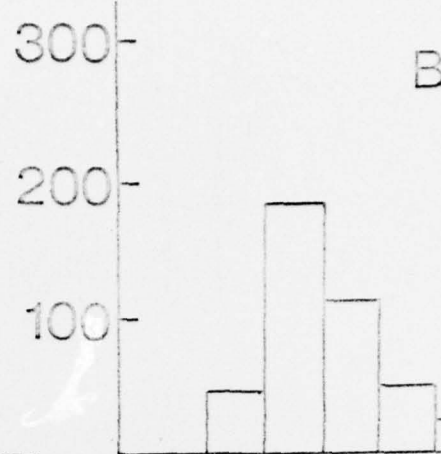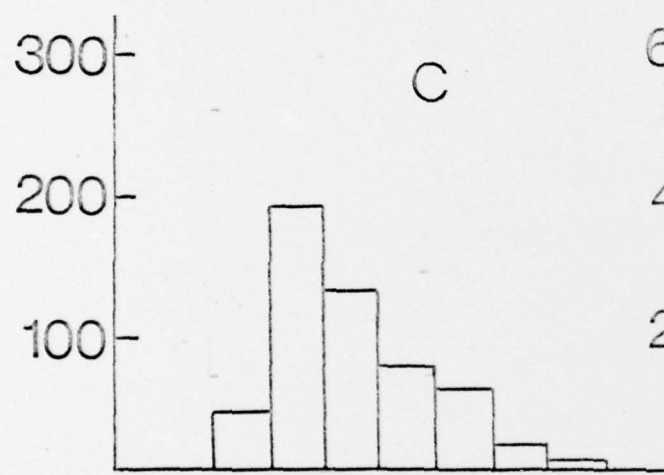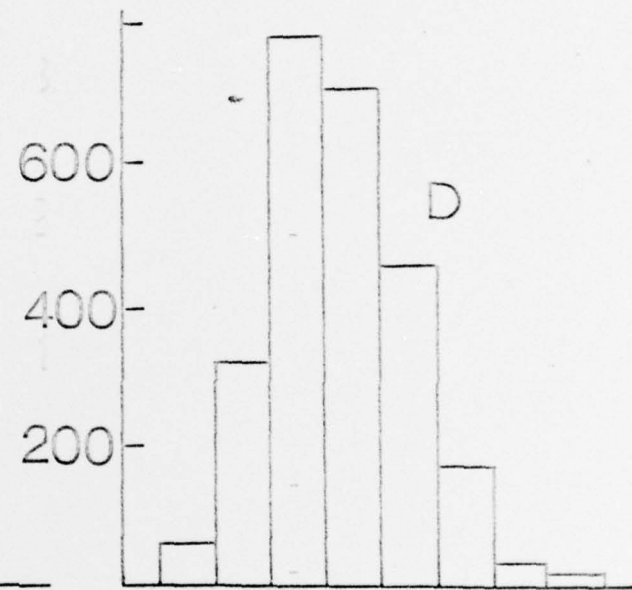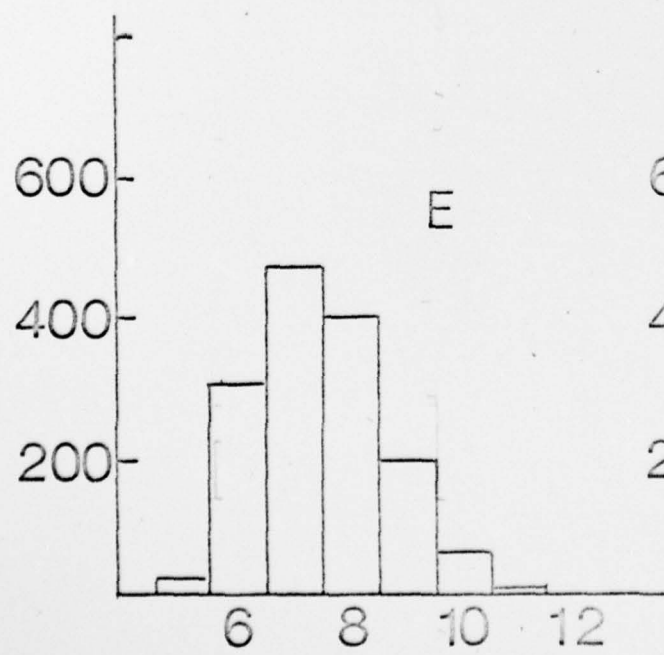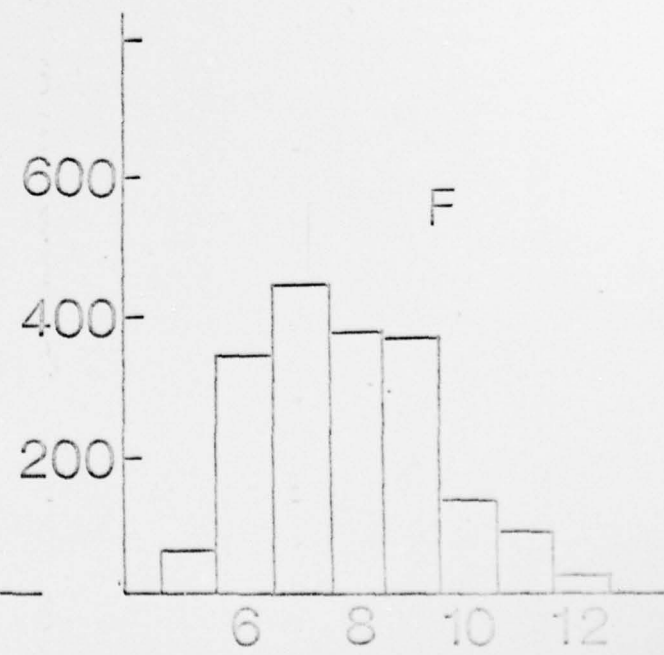
fig 3.3
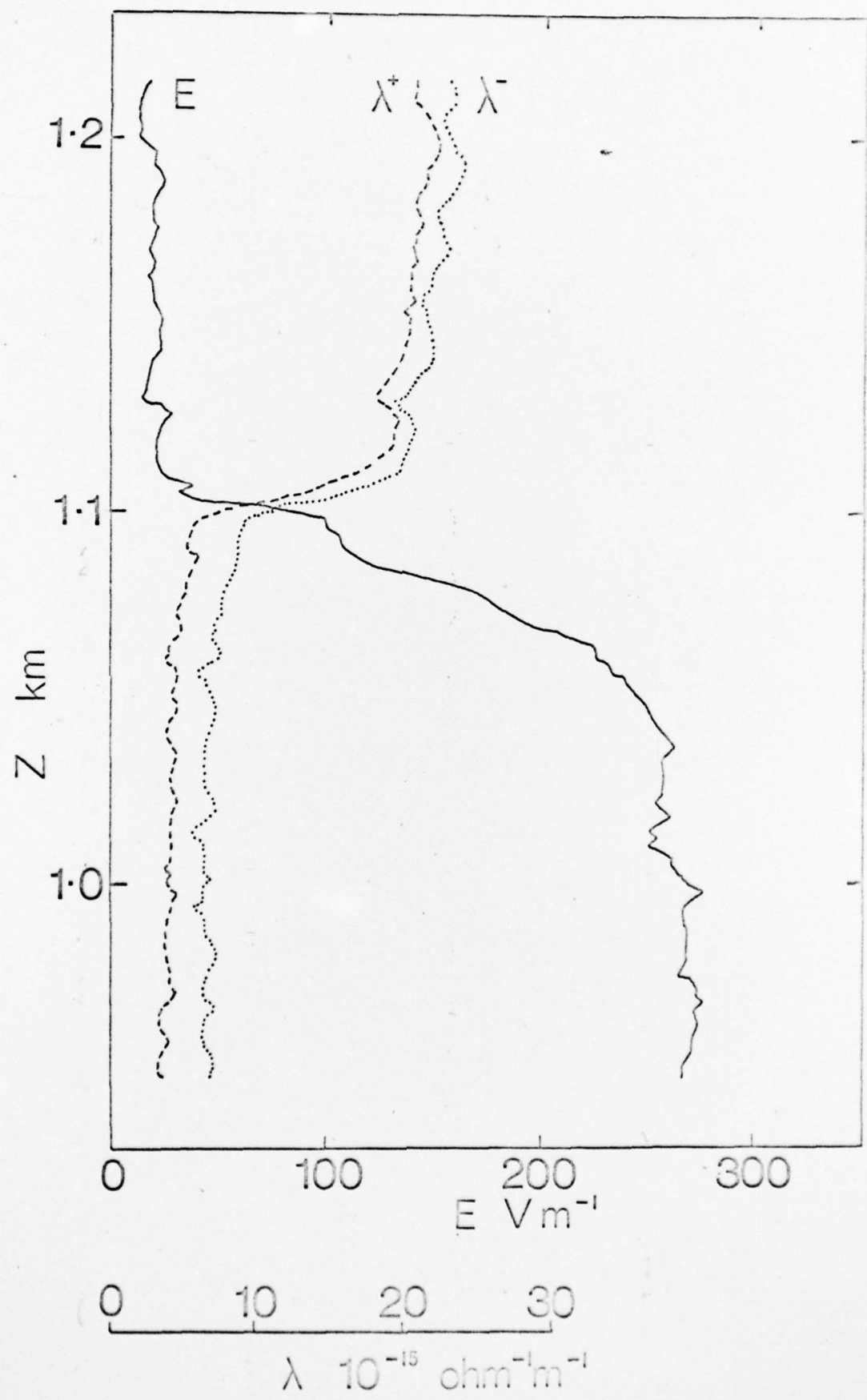
fig 4.1
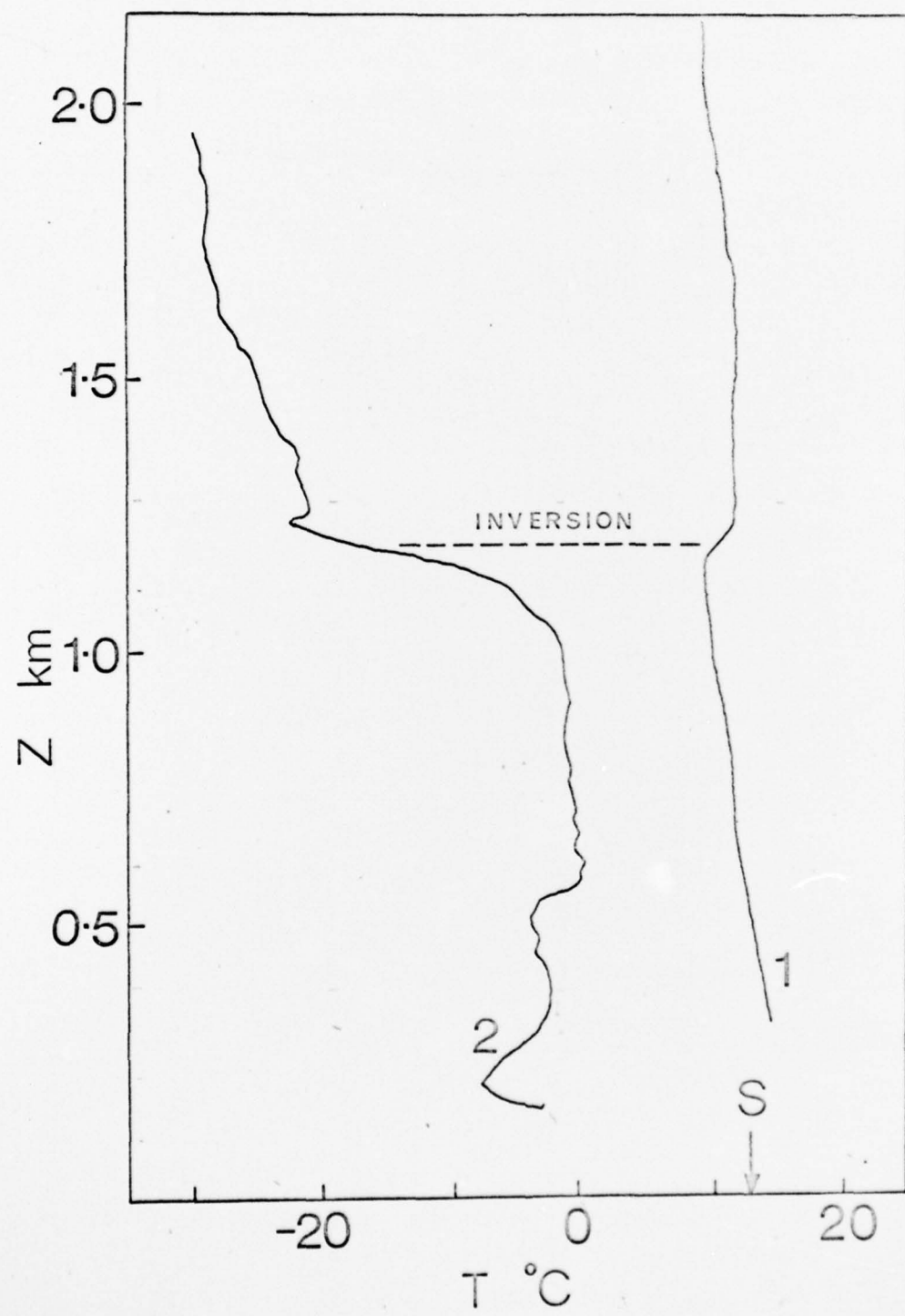
fig 4.2
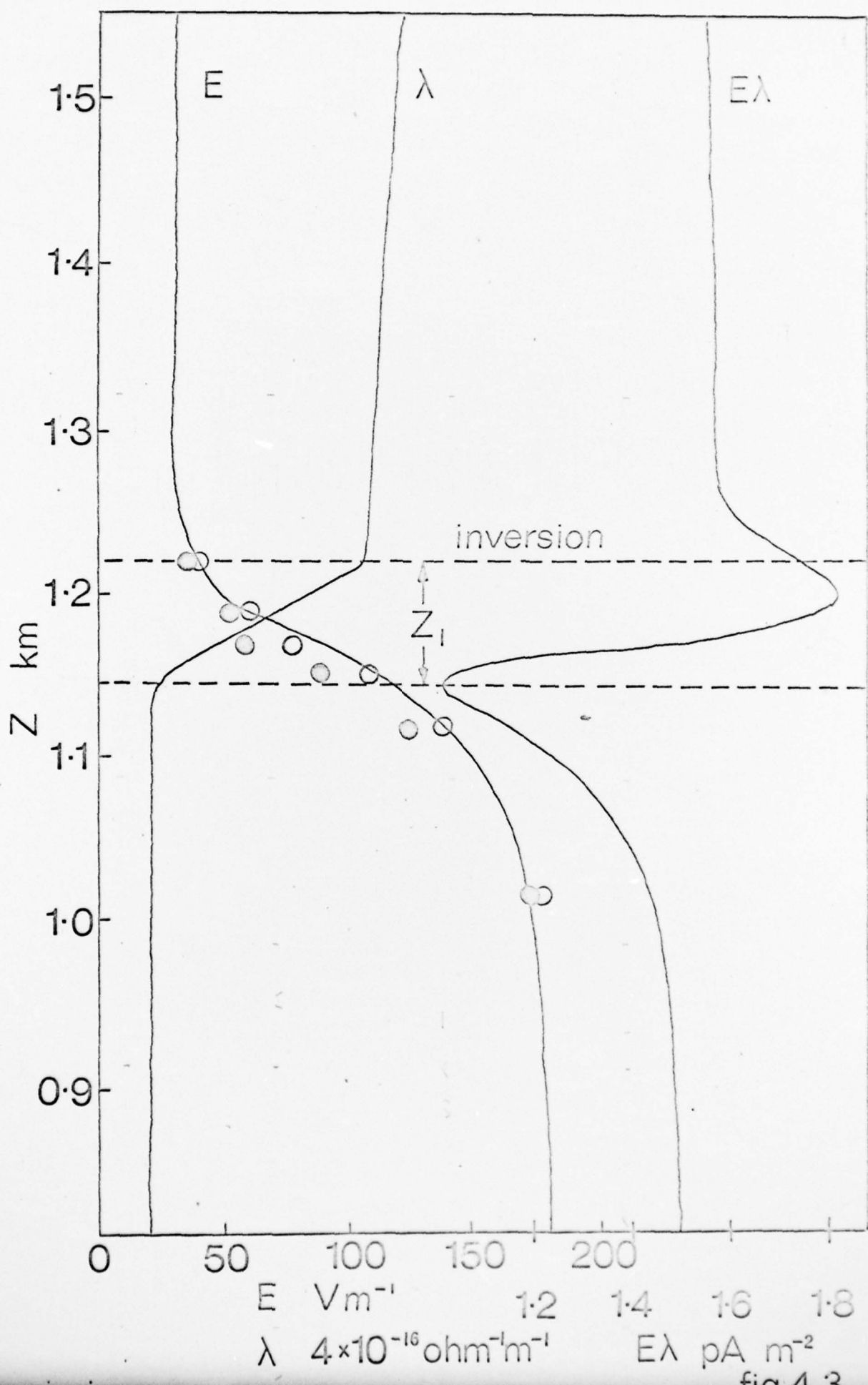
fig 4.3
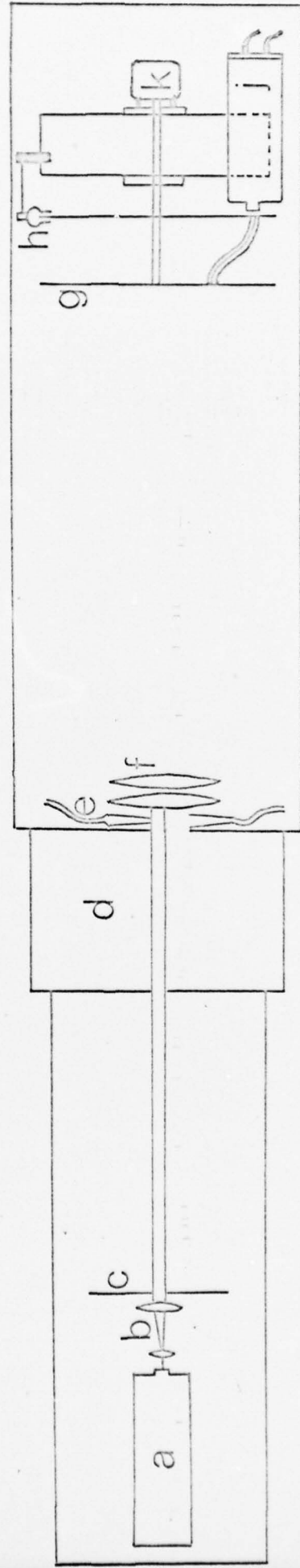
fig 5.1

Figure 5.2

THE INSTRUMENTED SAILPLANE